Biobased Chemistry and Technology

MSc Thesis Biobased Chemistry and Technology

Temperature control of microalgae cultivation under variable conditions

Elianne van Esbroeck

25-05-2018

WAGENINGEN
UNIVERSITY & RESEARCH

Temperature control of microalgae cultivation under variable conditions

Name course	:	MSc Thesis Biobased Chemistry and Technology
Number	:	BCT-80436
Study load	:	36 ects
Date	:	13-05-2018

Student	:	Elianne van Esbroeck
Registration number	:	931023229110
Study programme	:	MAB
Report number	:	096BCT

Supervisor(s)	:	dr. ir. AJB (Ton) van Boxtel
Examiners	:	dr. ing. RJC (Rachel) van Ooteghem
Group	:	Biobased Chemistry and Technology
Address	:	Bornse Weilanden 9 6708 WG Wageningen The Netherlands

Summary

Microalgae have the potential of becoming an important potential resource for different industrial applications, such as in food supplements, CO_2 capture, and wastewater treatment or as renewable energy source. There are different growth variables that need to be considered when trying to model microalgae growth. Many research studies focussed on controlling the variables: O_2, light, pH, CO_2, mixing and temperature to create the ideal conditions for microalgae with different control methods.

The current study focussed on temperature as the control variable on microalgae production. The control method used in the current research study was optimal control. The aim of the study was to find out how the optimal input trajectory changed under different circumstances. These different circumstances were created by making different scenarios. The different scenarios obtained location, season and variation during a day in a closed outdoor photobioreactor.

The model used in this research consisted of two models; temperature model from Fernández et al. (2014) and microalgae biomass growth model from Slegers et al. (2013b).The model was analysed and results showed that the model was a stiff system. The model was adapted by using pseudo-steady-state for the heater system. The proposed software Tomlab, turned out not to be suitable for this system because the results shown were unreliable. Optimization of piecewise linear trajectories showed results with a positive profit and a microalgae growth higher than in the uncontrolled system simulation. Therefore, piecewise linear trajectories was used to compare the optimal input trajectory with the different scenarios. The different scenarios contain two locations, three seasons and variation during a day. The locations Spain and the Netherlands were taken as potential grow location both having their own temperature and light intensity profile. To accurately model the temperature variation over the year, also seasonal variations are taken into account. The variation during a day is represented by a noise on the light intensity which resembling cloud coverage.

The results of the control input trajectories have a strong peak at the beginning of the day to get the ambient temperature until the optimal temperature, followed by cooling or heating depending on the ambient temperature. The days ends with a high peak. In general, the same peaks are observable in the control input trajectories for the different scenarios but in different sizes and on different moments. The peaks depends per scenario on the light availability and ambient temperature. The results show that in both locations the control input trajectory for the season spring resembles the control input trajectory for the season fall. In the location the Netherlands, the heating starts earlier due to the colder outdoor conditions. However, even though heating starts earlier the optimal temperature is reached later in comparison to the location Spain. In Spain, photo-inhibition plays a role.

In this research, with the price of microalgae being € 25/kg, cost of heating € 0.04/kWh and cost of cooling € 0.02/kWh, the cost function shows the highest profit for the summer in the Netherlands, namely € 150,27 per day. The costs for heating and cooling in all scenarios are approximately between € 31,- and € 54,- per day. The lowest profit of the six scenarios is also in the Netherlands, in the fall. All profits are positive indicating that with the price of microalgae and for heating and cooling taken in this case, it is profitable for the microalgae production to keep the temperature in the photobioreactor at an optimal temperature.

This study shows that the location and season in growing microalgae does contribute to the optimal input trajectory. When it comes to the day-to-day variation piecewise linear trajectories is not a suitable method to use, giving inaccurate results. Nevertheless, when it comes to locations and seasons, heuristic rules have been made for temperature control with piecewise linear trajectories.

Table of Contents

1 Introduction

Microalgae are becoming an important potential resource for different industrial applications. In these industrial applications, there are two different options possible; microalgae biomass can be the desired product or the metabolite. The microalgae biomass is used in food supplements or animal food, while the metabolite is for example used for pharmaceutical or nutraceutical applications, like vitamins or proteins. Other applications such as CO_2 capture, wastewater treatment or as a renewable energy source have also been observed. This shows the great potential of microalgae (Bernard, 2011; De la Hoz Siegler et al., 2012; Ugwu et al., 2008). The reason that microalgae stand out compared to other plants is their behaviour, which is predictable due to the interaction between biology (microalgae development and respiration) and physics (light attenuation and hydrodynamics) (Bernard, 2011).

There are different culture types in which microalgae can grow, under indoor and outdoor circumstances. The advantage of an indoor environment is the high level of controllability. However, this high degree of control makes the production of microalgae expensive. Placing microalgae production outside may be cheaper. This is, however, not always possible depending on the local climate conditions, since this affects the production. For example, the yearly outdoor areal biomass productivities for the microalga *P. tricornutum* in different reactors (raceway ponds, horizontal tubes, vertical tubes, flat panels) all have a higher biomass production in Spain compared to in the Netherlands (Slegers et al., 2011, 2013a, 2013b). Indicating that in the Netherlands microalgae production cannot reach the same amount of biomass concentration under outdoor conditions. However, it should be noted that the temperature in Spain is not ideal as well, since in the summer the temperature reaches such high levels that production is not possible without cooling the reactor. To make optimal conditions in both locations the production costs will increase, making the microalgae less interesting for the different industrial applications.

1.1 Microalgae growth variables

Microalgae growth is affected by various physical, chemical and biological factors. Factors that influence growth are for example light, energy supply, availability of CO_2, O_2-concentration, mixing, and control of environmental parameters like temperature (heating and cooling), pH and nutrients (Mehlitz, 2009; Suh et al., 2003).

To reduce the production costs, accurate operation, low-cost resources and optimization of the design will be important according to Fernández et al. (2014). Some examples to reduce costs are: coupling of microalgae production with combustion power plants or other CO_2 sources to sequester greenhouse gas emissions, utilizing nutrients from wastewater treatment facilities, or low quality water. When it comes to improving the design of the photobioreactor for optimal production, a lot of research has already been done. Optimization of the design can be achieved by selecting a certain type of algae and reactor, which determines the growth characteristics, appropriate for the cultivation conditions.

Worldwide there are two different cultivation systems used for the production of microalgae: open raceways ponds and closed photobioreactors. Open raceway ponds are basic cultivation systems. Biomass productivities in raceway ponds are low, there is a high risk of contamination and the production is highly dependent on the environment. However, open raceways ponds do have low construction and operating costs (Slegers et al., 2013b).In contrast to the open raceways ponds, the closed photobioreactor has more control of the cultivation conditions. There are different types of closed photobioreactors: tubular, flat and bubble column. There are a couple of advantages of the photobioreactor, but the main one is that higher biomass production is obtained and contamination is easily prevented. Although, one major setback of the closed photobioreactor is the lack of

efficiency with utilizing solar energy for biomass production. Other disadvantages of the closed photobioreactors are the high capital costs when it comes to controlling the conditions for the microalgae growth (Svaldenis, 2014; Ugwu et al., 2008).

To fully understand and later on control the productivity potential of microalgae, models must be constructed. Many growth kinetic models have been developed to describe the microalgae growth (Lee et al., 2015). The economic costs of algae cultivation are highly sensitive to the productivity of microalgae and to maintaining a steady operation. In literature, there are different articles that attempt to create optimal conditions, by controlling several factors. Most of these studies on optimization of microalgae cultivation are based on trial-and-error and/or design heuristics (Malek et al., 2015). As mentioned before, the microalgae growth is affected by various factors. In the following paragraphs, the effect of the factors O_2, light, pH and CO_2, mixing and temperature on microalgae production will be discussed by comparing available literature studies on how to control these factors and with which control methods.

Effect of O_2
During photosynthesis, O_2 is produced because microalgae, similar to plants, assimilate inorganic carbon into organic matter which produces O_2. The photosynthetic reaction is driven by energy from sunlight. Hu et al. (2012) developed a kinetic model to describe the dynamic characteristics of O_2 - concentration and its influence on the growth of microalgae in bioreactors. This was done in a closed-loop photobioreactor with a Linear-Quadratic Gaussian (LQG) servo controller, for O_2, which was optimized throughout simulation.

Effect of light
Light is needed for photosynthesis to occur, which can be supplied in different ways; natural light (sunlight) or artificial light. However, there are some disadvantages with both methods. Too much light intensity may result in photo-inhibition, which is light-induced reduction of growth (Béchet et al., 2013). Other phenomena that can occur with too much light intensity is overheating, which will cause the microalgae to perish. The duration of light in outdoor cultivation depends on the climate conditions, while at indoor conditions the light intensity can be altered with the use of artificial illumination.

Effect of pH and CO_2
The optimal pH range for microalgae is between seven and nine, although some species have a pH in a more acid or basic range. It is crucial to maintain the culture pH in the optimal range so that cellular process can continue. An acceptable pH can be accomplished by aerating the culture. In case of high density microalgae, the addition of carbon dioxide (pure CO_2 or high CO_2 flue gases), allows to correct for increasing pH (Wang et al., 2012). Model Predictive Control (MPC) in tubular photobioreactors for pH and solar radiation is done in order to achieve desired regulation properties and trying to minimise CO_2 losses (Berenguel et al. (2004). The same objective can be found in the study by Fernández et al. (2010), but the latter also indicates the issues that occur in modelling and controlling of the pH. Instead of the control method MPC Fernández et al. (2010) uses a Proportional–Integral (PI) control system with pulse width modulation (PWM) combined with a feedforward term to compensate for the solar radiation influence. Bernard (2011) focuses more on describing the hurdles and challenges for modelling and control of CO_2.

Effect of mixing
Mixing is an operation factor, which ensures that all cells of the population are equally exposed to light and nutrients. It avoids thermal stratification, improves gas exchange between the culture medium and the air, and prevents sedimentation. Mixing can be achieved by different methods, for example stirring by aerating, pumping, mechanical agitation (e.g. paddle wheels) or a combination of

these methods. The method which is used depends on scale and choice of the cultivation system (Wang et al., 2012).

Effect of temperature
Temperature is a measured environmental variable, and an important factor that affects the performance of microalgae growth. Every microalgae species has an optimal temperature, which is generally between 15 °C and 30 °C. This value may vary with the composition of the culture medium and the strain. When the temperature is below 15 °C microalgae growth will slow down, but when the temperature is higher than 30 °C microalgae growth will stop. Different control methods for control temperature are mentioned by Wang et al. (2012). This paper mentions the following control methods: shading of tubes with dark sheets, spraying of water when the culture temperature exceeds a certain value, submerging the entire solar tubes under water or installing a heat exchanger.

In conclusion, literature shows that there have been efforts done in controlling factors such as, O_2, pH, CO_2, mixing and temperature or a combination of these factors, in order to optimize production of microalgae. In the paper by Guterman et al. (1990), the following parameters were controlled; light intensity, optical density, pH and temperature on microalgae growth. An on-line optimization and control procedure was used. Another article which uses also more than one control factor is De la Hoz Siegler et al. (2012). In this article, the focus lies on optimization of biomass and oil production using an adaptive, non-linear model. For parameter estimation, off-line measurements of the carbon source and biomass concentrations were used. Using of an algorithm, the optimal strategy was recalculated by means of a shrinking horizon approach. These articles show that model based optimization is a valuable tool for improving the economic performance of microalgae production.

Optimizing microalgae production is done with different control methods. However, optimal control is rarely applied. Van Straten et al. (2010) is one of the few who uses optimal control. In his paper, the control variable is the dilution rate, and light intensity is taken as external input. However, next to light, temperature is the most important limiting factor in outdoor systems. The effect of temperature on laboratory scale is well documented, but the effects in outdoor conditions are not yet sufficiently documented (Mata et al., 2010). Therefore, in this research temperature was chosen as control variable. As external inputs, ambient temperature and light intensity in an outdoor closed photobioreactor were chosen. In outdoor cultivation systems, the light intensity and ambient temperature will vary with time and per location. Ambient temperature is generally low in winter and high in summer, therefore requiring temperature regulation (heating and cooling), to create a continuous optimal temperature condition for the microalgae to grow. Heating and cooling will create additional costs. Therefore, a trade-off should be made between the costs of heating and cooling and the additional biomass that will be produced. Hence, the control objective is to efficiently use the sunlight and ambient temperature associated with the circumstances of the location to increase the biomass production as much as possible without increasing the energy costs. In optimal control, the control objective focuses on how to calculate the control input in such a way that the controlled system shows a desired behaviour.

1.2 Research aim

The aim of this research is to find the optimal input trajectory that satisfies the control objective. The optimal input trajectory will show the optimal temperature setting throughout time, with the intention to make optimal use of the outdoor temperature and light conditions in different situations. The outdoor conditions will depend on different factors. In this research, the focus is on the following factors: variation during a day, location and season. This because the daily passage of the sun together with local weather, for example cloud coverage, influence light intensity and the ambient temperature. The location of the photobioreactor is a critical factor for the amount of light.

The efficiency of the photobioreactor depends on the local climate and therefore the location significantly contributes to the cultivation. The locations chosen are Spain and the Netherlands. To accurately model the temperature variation over the year, also seasonal variations are taken into account. Considering the aforementioned variables, the effects of weather disturbances on the optimal input trajectory should become more visible. It is hypothesised that for the location in Spain more cooling would be necessary compared to the location in the Netherlands, making the cooler seasons in Spain more preferable.

1.3 Research questions

The following research questions will be addressed in this research.

- What is the optimal input trajectory for a standard situation?
- How is the optimal input trajectory affected by the variation during a day, location and season?
- Is it possible to translate the optimal control strategies for different situations into heuristic control rules?

1.4 Approach

In order to answer the research questions the following approach will be applied: a closed tubular photobioreactor system with degassing and a heat exchanger will be used. In order to simulate what happens in an outdoor closed photobioreactor, the growth model from Slegers et al. (2013b) and the dynamic model from Fernández et al. (2014) will be combined. When the model is designed, optimal control will be applied to calculate the optimal input trajectory for a certain temperature and light intensity to create a standard situation. After this, the different variations; variation during a day, locations and seasons, will be added. The optimal input trajectories will be calculated to evaluate how the trajectory is affected by the different variables. These results will be analysed and evaluated to see if it can be translate into heuristic control rules for the different situations.

2 Fundamental models

The following chapter gives details on the equations and parameters of the temperature model from Fernández et al. (2014) and the microalgae production model from Slegers et al. (2013b) that is used in this research. The purpose of using these models is to get an accurate representation of what happens in an outdoor closed photobioreactor. The model that is described will exist of two mathematical models, the temperature model and biomass model with ambient temperature and light intensity as disturbances inputs depending on the climate conditions and the temperature as control variable. The model in this research will provide information on how the temperature distribution and the biomass production behaves with different ambient temperatures and light intensities.

In this chapter, first both models will be explained and analysed. Next, optimal control will be explained, as this is the method used to calculate the optimal control input trajectory. Finally, the different scenarios that were made will be given. The model equations and microalgae characteristics are developed from literature and coded in Matlab and Tomlab.

2.1 Materials

In this research, the microalga *T. pseudonana* was used, which has an optimal temperature of 24.73 °C (Slegers et al., 2013b).When the temperature exceeds the optimal temperature, the microalgae growth rate decreases. This decrease can generally be explained by heat stress. A bell-shaped growth curve is observed for describing temperature response of microalgae growth rate (Ras et al., 2013). Next to the optimal temperature, the microalga also has a lethal temperature, which is for this type of microalga 31.40 °C (Slegers et al., 2013b).The biomass production will not take place when the temperature is above the lethal temperature. In this research, the focus lies on optimal control influencing the temperature of the reactor. Because of this focus, the pH is assumed to be ideally controlled at a level considered optimal for the microalgae studied. However, besides the pH and carbon supply, microalgae also need nutrients to grow and reproduce. An example of these nutrients are nitrogen and phosphorus (Mehlitz, 2009), which are assumed to be non-limiting to the microalgae growth in this research.

2.2 System description

In this research a closed photobioreactor is used (Figure 2-1), which shows the functioning of the system. The photobioreactor exists of two different parts: the bubble column and the tubes, also known as solar receivers. The tubes (solar loop) are designed to collect the solar radiation as efficient as possible and minimize resistance of the culture flow. In the bubble column a heat exchanger is located together with a degasser (Berenguel et al., 2004). In this part of the reactor, perfect mixing is assumed. From the bubble column the circulation moves through the tubes (in an upwards direction). The assumption is that the tubes are laying down, so the effect of shadowing does not apply to this situation. The culture temperature can be controlled by the heat exchanger, which is situated in the bubble column, by passing water through it. Heat balances are made for the tubes, the bubble column and the heat exchanger. These heat balances take both fluid-dynamics and heat transfer phenomena into account. The assumption is that the ambient temperature surrounding the photobioreactor is uniform (Fernández et al., 2014).

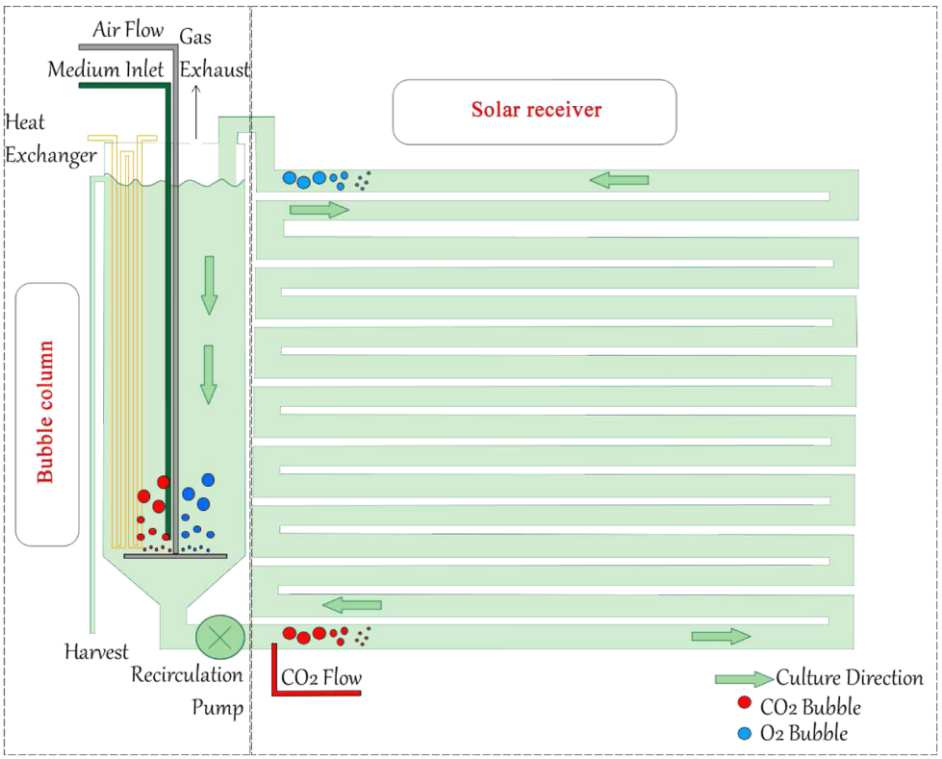

Figure 2-1: Schematic representation of the closed photobioreactor (from Fernández et al. (2014))

2.3 Temperature model

In the paper of Fernández et al. (2014), a first principles model of a tubular photobioreactor for microalgae production is given. This model represents the physiochemical and biological phenomena that take place inside the photobioreactor. The temperature model considers the following variables: light availability, culture conditions, mixing and gas-liquid mass transfer. In outdoor cultures, the light irradiation and temperature availability depends on the location where the photobioreactor is positioned. The following paragraphs will give the equations about the different parts (tubes, bubble column and heat exchanger) of the photobioreactor.

2.3.1 Photobioreactor tubes

The main part inside the photobioreactor where the microalgae can grow are the tubes. The temperature inside the tubes will depend on different variables. The solar radiation will heat up the tubes, some heat will be lost to the ambient air, and the rest of the heat will arrive from the bubble column. The culture moves through the tubes, making it a distributed system, with different temperature and biomass on different positions in the tubes. The tubes of the closed photobioreactor are designed to collect solar radiation as efficiently as possible. The length of the tubes can differ; longer tubes means a larger absorption of solar radiation. However, longer tubes causes more heat exchange with the ambient air. This will all depend on the design of the photobioreactor. The following equation (Eq. 2.1) is used to describe the heat balance in the tubes, which takes the design variables into account. When the total length of the tubes is divided into n number of pieces, equation 2.1 will hold for one piece of tube.

$$\frac{\partial T(t,x)}{\partial t} = \frac{\left(-Q_{liq,t}(t,x)\ C_p\ \rho \frac{\partial T(t,x)}{\partial x} + \alpha_t\ I_0(t)\ \pi\ d_t\ a\ \partial x + h_t\ \pi\ d_t\ \partial x\ \left(T_{amb}(t) - T(t,x)\right)\right)}{\pi \frac{d_t^2}{4}\ \partial x\ C_p\ \rho} \quad (2.3.1)$$

With $Q_{liq,t}$ ($m^3\ s^{-1}$) the volumetric flow rate of liquid in loop, C_p (J kg^{-1} $°C^{-1}$) the heat capacity of the growth medium, ρ (kg m^{-3}) the volumetric mass density, T (°C) the temperature of the culture, ∂x (m) total length of the tubes divided by the n number of pieces, I_0 (W m^{-2}) the solar irradiation which is modulated by a distribution factor called α_t (-), d_t (m) the loop diameter of the tubes, a (-) a constant which represents the solar irradiance absorptivity, h_t (J s^{-1} m^{-2} $°C^{-1}$) the coefficient of heat transmission between the ambient and the culture temperature and T_{amb} (°C) the ambient temperature, which is considered homogeneous in the space around the tubes (Fernández et al., 2014).

With Equation 2.3.1, the temperature variations in time can be calculated at different places in the tubes. The culture moves through the entire tube and ends in the bubble column. In the bubble column, perfect mixing is assumed. The following subchapter goes into detail on the differential equation of the bubble column.

2.3.2 Photobioreactor bubble column

The bubble column is positioned next to the tubes (solar receiver) in the photobioreactor. The bubble column contains a heat exchanger. The differential equation for the bubble column is given in Eq.2.2. The heat difference between inlet and the outlet of the bubble column, the solar radiation heating the bubble column, the heat loss with the ambient air, and finally the heat increase due to the heat exchanger all these variables influence the temperature in the bubble column.

$$\frac{\partial T_{out}(t)}{\partial t} = \frac{\left(-Q_{liq,b}(t)\ C_p\ \rho\ \left(T_{out}(t) - T_{in}(t)\right) + \alpha_b\ I_0(t)\ S_b\ a + h_b\ S_b\left(T_{amb}(t) - T(t)\right) + h_{ext}\ S_{ext}\left(T_{ext}(t) - T_{out}(t)\right)\right)}{\left(C_p\ \rho\ V_{liq,b}(t)\right)} \quad (2.3.2)$$

With $Q_{liq,b}$ ($m^3\ s^{-1}$) the volumetric flow rate of liquid in the bubble column, T_{in} (°C) and T_{out} (°C) are the culture temperature at the inlet and outlet of the bubble column, α_b (-) is the light distribution factor in the bubble column, h_b (J s^{-1} m^{-2} $°C^{-1}$) is the coefficient of heat transmission to the ambient in the bubble column, S_b (m^2) is the column area available, h_{ext} (J s^{-1} m^{-2} $°C^{-1}$) is the coefficient of heat transmission between the heat exchanger situated in the bubble column and the culture temperature, S_{ext} (m^2) is the heat exchanger area, T_{ext} (°C) is the temperature in the heat exchanger and $V_{liq,b}$ (m^3) is the liquid bubble column (Fernández et al., 2014).

The temperature derived from the heat exchanger is the average between the temperature that comes out of the heat exchanger and the temperature that comes in. How the heat exchanger temperature that comes out and into the bubble column is calculated can be seen in the following subchapter.

2.3.3 Photobioreactor heat exchanger

The last temperature heat balance is the one of the heat exchanger. Here the heat that comes out of the heat exchanger during a certain amount of time is defined by the difference between the heat that comes into and moves out of the heat exchanger, together with the difference between the

average heat exchange temperature and the temperature in the bubble column. This is given in the following equation (2.3.3).

$$\frac{\partial T_{ext,out}(t)}{\partial t} = \frac{\left(-Q_w(t)\ \rho\ C_p\ (T_{ext,out}(t) - T_{ext,in}(t)\ -\ h_{ext}\ S_{ext}\left(T_{ext}(t) - T_{out}(t)\right)\right)}{(C_p V_{ext})} \quad (2.3.3)$$

where Q_w ($m^3\ s^{-1}$) is the volumetric flow rate of water that crosses through the heat exchanger, $T_{ext,in}$ (°C) and $T_{ext,out}$ (°C) are the culture temperature at the inlet and outlet of the heat exchanger and V_{ext} (L) is the total volume of the heat exchanger (Fernández et al., 2014).

All these equations are used for calculating the temperature in the tubes, bubble column and the heat exchanger.

2.4 Microalgae biomass growth model

In previous chapters is explained how various factors influence the overall microalgae growth. More information on the growth kinetics of the microalgae can be found in appendix A. In the previous subparagraph is explained how the photobioreactor is build up, and what the temperature circumstances are in the photobioreactor. These subparagraphs will move into details about the microalgae growth, and how this is influenced by light intensity and temperature.

The dynamics of the biomass concentration over time (t) and space (x) are given by:

$$\frac{dC_x(t,x)}{dt} = \left(\mu_{growth}(t,x) - r_m(t) - D(t)\right) C_x(t,x) \quad (2.4.1)$$

with C_x ($kg\ m^{-3}$) the biomass concentration, μ_{growth} (s^{-1}) the specific growth rate, D (s^{-1}) the dilution rate over a period of time, and r_m (s^{-1}) the maintenance metabolic coefficient, also known as respiration rate (Slegers et al., 2013b).
The growth rate depends on light intensity and temperature with respect to time and place.

$$\mu_{growth}\ (t,x)\ = f\left(I(t), T(t)\right) \quad (2.4.2)$$

With $I(t)$ being the light intensity and $T(t)$ being the culture temperature. In the following subparagraphs, the light distribution and the temperature distribution are explained in more detail.

2.4.1 Effect of light distribution

In the photobioreactor, microalgae are able to grow inside the tubes or the bubble column. In these locations, light will fall on the material, which can be reflected, absorbed and transmitted. For simplicity, the effect of light scattering on the material was neglected. Microalgae can absorb part of the light, which limits their own growth. In addition, during the night the population density of microalgae decreases due to respiration and the lack of light (Chisti, 2007).
Light intensity will decrease along the path length of a closed photobioreactor. The law of Lambert-Beer can be used to calculate the average light intensity at each location within the microalgae culture (Hermanto, 2009).

At low densities within the reactor, the intensity of light will increase exponentially according to the Lambert-Beer law (Quinn et al., 2011). The Lambert-Beer law can be described as follows.

$$I\ (L) = I_0(t)\ exp\big(-K_a\ C_x(L)\big) \tag{2.4.3}$$

Where I (µmol m^{-2} s^{-1}) is the amount of light available at distance L (m), I_0 is the light intensity incident on reactor wall, C_x (kg m^{-3}) is biomass concentration where the light intensity reaches, and the variable K_a (m^2 kg^{-1}) is the specific light absorption coefficient, which is a specific parameter of the algae species.

At higher densities, scattering is important to consider for determining local light intensity according to Quinn et al. (2011). In this model, an average light intensity in the reactor was calculated with the following equation.

$$I_{av}(t,x) = I_0(t)\ \alpha\ \frac{1-exp\ \left(-K_a\ C_x\ (t,x)\ \frac{d_p}{2}\right)}{K_a\ C_x\ (t,x)\ \frac{d_p}{2}} \tag{2.4.4}$$

Where t presents time, x is the space, I_0 is the solar irradiation on an obstacle-free horizontal surface, K_a (m^2 kg^{-1}) is the specific light absorption coefficient, C_x (kg m^{-3}) is the biomass concentration, and d_p (m) is the tube diameter in the p part (where p can be substituted by 't' for the tubes and 'b' for the bubble column). The diameter is divided by two because the light intensity comes in from two different sides. The solar irradiance can be modulated by a distribution factor α, which represents the solar irradiance fraction available in a particular area of the reactor. This factor becomes important for the light loss when placing the photobioreactor inside a greenhouse (Fernández et al., 2012).

The equations above can be used to establish the light gradient inside the tubes or bubble column. To calculate the light inside the bubble column, the diameter and the biomass concentration need to be adapted. During photosynthesis, microalgae only use the visible fraction of the light. This fraction is better known as photosynthetically active radiation (PAR). In sunlight, PAR accounts for approximately 43% of the total spectrum (Lösing, 2011). The sunlight (light irradiance) used in this model is expressed in W/m^2. However, a conversion is needed to photosynthetic photon flux density I_{PFD} (µmol photons/m^2 s), which can be done by a conversion factor of 4.56 µmol/J (Langhans et al., 1997). For the temperature model, the light intensity was expressed in Einstein unit (µE/m^2). However, when only considering the visible fraction of light (PAR, 400-800 nm), the Einstein unit is equal to µmol photons/m^2 s (Langhans et al., 1997). This conversion occurs as photochemical reactions are based on the number of photons involved. Therefore, the light energy in µmol photons/ m^2 s that is available for microalgae photosynthesis is giving in the following equation.

$$I_{FPD} = 0.43 * 4.56 * I_{av}(t, x, C_x, d_p) \tag{2.4.5}$$

2.4.2 Effect of temperature on growth

In this research, the model accounts for the effect of temperature on microalgae growth through the following equation. When considering a seasonal and daily cycle, temperature is the environmental factor that consistently accounts for the largest part of the variance in growth (Quinn et al., 2011).
This temperature modelling is expressed with the variable f_T (-), which is a dimensionless number between zero and one. This model assumes that the temperature affects the photosynthesis rate (Geider et al., 1997). The temperature factor is given in the following equation.

$$f_T = \left(\frac{T_{let} - T_{(t,x)}}{T_{let} - T_{opt}}\right)^{\beta_T} exp\left(-\beta_T \left(\frac{T_{let} - T(t,x)}{T_{let} - T_{opt}} - 1\right)\right) \quad (2.4.6)$$

In Eq.(2.4.6), the lethal temperature is represented by T_{let} (°C), T_{opt} (°C) is the optimal growth temperature, and β_T (-) is the curve modulating constant. All these variables are dependent on the type of algae species. $T(t,x)$ (°C) is the culture temperature at a certain space and time. The temperature factor f_T (-) represents the influence of the culture temperature on the microalgae growth. The f_T increases when the temperature increases up to an optimal temperature, and then decreases gradually, while varying between zero and one.

2.4.3 Growth rate

In literature there are different mathematical models given for the growth of microalgae. The most known models are Monod model or Droop model. A growth model gives an estimation of the algae growth under dynamic light conditions. As seen in equation (2.4.1), the change in biomass concentration is dependent on the specific growth rate, dilution rate, and metabolic maintenance coefficient. The growth rate model used in this research is based on Slegers et al. (2013b) which uses a growth model developed by Geider. In this model, the photosynthetic activity of the microalgae and the chlorophyll a:carbon ratio is connected, which is irradiance dependent. The growth rate is described by the following equation:

$$\mu_{growth}(t) = P_m^c \left(1 - exp\left(\frac{-\alpha_{photo}\, I_{PFD}(t,x)\, \Theta_a(t,x)}{P_m^c}\right)\right) \quad (2.4.7)$$

Where P_m^c (s^{-1}) is the maximum carbon specific rate of photosynthesis, the functional cross section of the photosynthetic apparatus α (g C (mol^{-1} photons) m^2 g^{-1} Chl a), the photon flow density I_{PFD} (µmol m^{-2} s^{-1}) and Θ_a (g^{-1}Chl a g^{-1} C), which is the chlorophyll a:carbon ratio (Slegers et al., 2013b).

The functional cross section α is used as a constant and the photon flow density depended on the outdoor conditions. The following equations show the calculation of the other variables presentation in the previous equation. The first equation gives the chlorophyll a:carbon ratio.

$$\Theta_a(t,x) = \Theta_{a,max}\left(\frac{1}{1 + \frac{\Theta_{a,max}\ \alpha_{photo}\ I_{PFD}(t,x)\ a}{2\, P_m^c}}\right) \quad (2.4.8)$$

Where $\Theta_{a,max}$ (g^{-1}Chl a g^{-1} C) is taken as a constant dependent on the microalgae species. The maximum carbon specific rate of photosynthesis can be calculated with the following equation:

$$P_m^c = \mu_{max}\, f_T + r_m \quad (2.4.9)$$

The maximum carbon specific rate of photosynthesis depends on the maximum specific growth rate μ_{max} (s^{-1}) and the maintenance metabolic coefficient r_m (s^{-1}).

All these formulas are used to calculate the expected biomass concentration with a certain light intensity and ambient temperature. However, when it comes to the biomass production inside the tubes, the biomass concentration not only depends on time but also on the place in the tubes. Inside the bubble column this is not the case, because perfect mixing is assumed. Therefore, the culture

temperature when calculating the biomass concentration for the tubes and bubble column differ from each other. The biomass concentration in the tubes is calculated with the culture temperature and light intensity of the tubes. The biomass concentration in the bubble column is calculated with the temperature and light intensity of the bubble column.

In appendix B, an overview of the model parameters with the specific assumptions are presented.

2.5 Analysis of the temperature model and the microalgae biomass growth model

In this research two mathematical models, namely temperature model (chapter 2.3) and biomass production model (chapter 2.4) are used and combined into one new model.

In the temperature model, three different heat balances (tubes, bubble column and heat exchanger) are considered. The heat balance for the solar receiver is formulated through partial differential equations (PDE). This gives a distributed description of the process in the form of a plug flow. The second heat balance is the differential equation for the bubble column. This is considered a stirred tank that is perfectly mixed and is modelled by an ordinary differential equation (ODE). The third heat balance is the heat balance for the heat exchanger, which is also an ODE.
In the microalgae biomass growth model, the main equation which represents the dynamics of the biomass concentration is an ODE. The specific growth rate, which is the first term of the ODE, can be calculated with different algebraic equations (equation 2.4 – 2.10).

Analysis of mathematical models.
Analysis of the properties of the mathematical models gives an indication of the behaviour of the system. Analysis of mathematical models can be done in different ways for example through steady state, equilibriums, or eigenvalue analysis. The stability of an equilibrium can be calculated by eigenvalue analysis (Van Boxtel, 2016).The eigenvalue contains a real and a complex part. The real part of the eigenvalue determines the 'speed' of the response; $e^{\lambda_{Re}\, t}$. Where $\lambda = \frac{1}{\tau}$, and therefore $\tau = \frac{1}{\lambda}$, where τ represents the time the system needs to respond. This system is non-linear, therefore linearization should be done for the states at equilibrium point. Another crude method to compare orders of magnitudes would be to write each differential equation in the form of:

$$\frac{dx_1}{dt} = f(.)x_1 + \cdots \rightarrow \tau_1 \approx \frac{1}{f(.)} \qquad (2.5.1)$$

In this system, the amount of differential equations is quite large and becomes complicated because of the exponents in the microalgae growth model. Therefore, it was chosen to calculate the response time for the different parts of the system. In the temperature model, the three heat balances describe the tubes, bubble column and the heat exchanger, respectively. The flow moves through the tubes, which has a length of 80 meter and the culture is circulated with 1 m/s using a centrifugal pump. Meaning that the response time in the tubes will be 80 seconds. The length of the bubble column is, 3.2 meter, giving the response time for the bubble column equal to 3.2 seconds. It is known that the heat exchanger is positioned in the bubble column and has approximately have the length of the bubble column. This results in a response time for the heat exchanger of 1.6 seconds.

The microalgae growth rate is described in the unit per second. It is known that the growth rate depends on the temperature and light intensity, but the maximum growth rate for this type of microalgae is equal to $3.81 \cdot 10^{-7}$ (s^{-1}) (Slegers et al., 2013b).

The result of this analysis shows that the system is stiff. A system is stiff, when one of the equations moves significantly faster than the other system. From the different response time is it visible that the heat exchanger is the one with the highest response time. A stiff system can be resolved in different ways. One way is by a pseudo-steady state. This is an assumption that models a small portion of the complex system, which contains both a slow and fast reaction. In this system, the slow reaction is the reaction in which you are interested is the microalgae biomass production. Moreover, the differential equation with the heat exchanger is the reaction with the highest response time compared to the other reactions. To apply pseudo-steady-state, the fast reaction is assumed in a state of dynamic equilibrium and their derivatives are equal to zero, compared to the other reaction (Mott et al., 2000). Therefore, this accumulation is put equal to zero. As the heat exchanger was placed in the bubble column, a term in the differential equation for the bubble column represents the heat exchanger. After applying pseudo-steady state, this term is replaced with Q.

2.6 Optimal control

There are different types of mathematical models that can be applied for optimization. All these methods calculate a certain trajectory for the input. In this research optimal control, also known as dynamic optimization is applied on the model. This optimization method finds an optimal solution for a quantitative mathematical system. The algae growth is a continuous dynamic system. The dynamics are described in terms of a state space model, given in the equation below:

$$\frac{dx}{dt} = f\ (x(t), u(t), d(t), p, t) \tag{2.6.1}$$

with x being a vector of state variables (in this case; temperature in tubes and bubble column, biomass concentration in tubes, and biomass concentration in the bubble column), d is a vector of disturbance variables (in this case; outside air temperature and light intensity), p is a vector of the parameters of the model, u is a control vector (in this case; power), t stands for time and f is a vector function. Both the control variables and the disturbances are time-varying.

For optimization of a system, a control objective is defined in the form of a cost function, which can either be minimized or maximized. The cost function is a result of the state variables at the final time and the running costs (Arthur E. Bryson, 1999). The cost function J is defined as follows in equation (2.6.3):

$$J = \Phi\left[x(t_f)\right] + \int_{t_0}^{t_f} \mathrm{L}\ (x(t), u(t), d(t), p, t)\ \mathrm{dt} \tag{2.6.2}$$

Where the first term on the right hand side of equation 2.6.2, represents the terminal conditions and the second term the running costs, with the start time t_0 and final time t_f, and initial conditions $x(t_0)$ specified. Maximization of the cost objective is equal to minimization of the cost function multiplied by a factor -1. The optimization problem involves the determination of the control input,$u(t)$ which maximizes or minimizes the performance criterion J for the given disturbance inputs. The choice of control input is limited to a feasible region, defined by constraints of the control, constraints of intermediate variables, and constraints of state variables (Van Willigenburg, 2017).

In this research, the goal of microalgae cultivation is to gain the maximal mass of harvested microalgae with the lowest costs for production, which is given by the following cost function J:

$$J = -w_1 \, price_{algae}(C_{x_{biomass}}(t_f) - Cx_0) \, Volume \; + w_2 \int_{t_0}^{t_f} (cost_{cooling} + cost_{heating}) \qquad (2.6.3)$$

With w_1 and w_2 representing the weight factors which can be added in order to make a distinction. The price of the algae will depend on the market value. In the equation, the produced biomass concentration is corrected for the initial condition. The costs are calculated by the amount of energy needed to keep the production at a certain level, either by cooling or heating.
In this case, the optimal control problem has inequality control constraints.

$$u^{min} \leq \; u(t) \leq u^{max} \qquad (2.6.4)$$

This to indicate the maximal and minimal power needed to cool or heat the photobioreactor. In case of optimal control, adding an additional state variable which was previously the running costs is better known as the Mayer formulation (Arthur E. Bryson, 1999). By applying the Mayer formulation in this system, an extra differential equation is added to present the running cost. The system behaviour is determined by $x(t)$, which is influenced by the disturbance inputs and control $u(t)$. The solution of the system will be found by finding the optimal control trajectory u_{opt} for which $J = J_{opt}$.

To solve constrained minimisation problems, Lagrange theory is applied. This theory transforms the constrained function minimisation problem into an unconstrained function, thus minimising the problem by multiplying each constraint with a Lagrange multiplier. A vector of Lagrange multipliers is also called a co-state. With introducing the Lagrange multiplied running costs of the cost function J, a new formulation will be created, also known as the Hamiltonian function.

$$H(x, u, t) = \; L(x, u, t) + \; \lambda^T \, f(x, u, t) \qquad (2.6.5)$$

The cost function is now changed into a functional. To find a local minimum of a functional, instead of considering partial first derivatives which all have to be zero, it is considered to be very small. The new cost function with the Hamiltonian part in combination with the Leibniz's rule will lead to the following co-state equation (Van Willigenburg, 2017).

$$\dot{\lambda^T} = \; -H_x \equiv -L_x - \lambda^T f_x \qquad (2.6.6)$$

Optimality is then achieved when $\lambda^T(t_f) = \; \phi_x \, (t_f)$ and $H_u = 0$ for $t_0 \leq t \leq t_f$. In the software application Tomlab, this optimization method is applied. An alternative method would be to use piecewise linear trajectory. Hereby, the day is divided into i intervals with linear increasing/decreasing energy input. The values of Q at the beginning of the day and at the end of each interval are the parameters to be optimized. The control input Q is given by the following equation:

$$Q = \big(t - t(i-1)\big) * \frac{u(i) - u(i-1)}{t(i) - t(i-1)} + u(i-1) \qquad (2.6.7)$$

Q can be either have a positive or negative value, respectively indicating if the control input is heating or cooling. The constraints placed on the system are that the heater cannot reach values higher than $1 \cdot 10^6$ (J/s) and for the cooler not lower than $1 \cdot 10^{-6}$ (J/s). The Matlab function fmincon is used to find the optimal input trajectory.

2.7 Scenario's

The growth model for an outdoor closed photobioreactor is used to simulate growth under different environmental and system conditions. The following circumstances are investigated: weather types (seasons and variation during a day) and locations. The model is simulated for outdoor conditions, whereby the climate influences the outcome of the optimal input trajectory. In this subchapter, a description is given of the following circumstances that were chosen and tested.
First, a reference system was made. However, to really test the model and to come up with optimal input trajectories for different situations, different scenarios have to be made. In this following chapter, the different scenarios that were made are explained.

2.7.1 Locations and seasons

In the model, one of the disturbance inputs is light irradiance, which is represented as average light intensity calculated based on light intensity at the reactor surface. This light intensity is mimicked by the positive values of a sine wave, which corresponds with outdoor conditions. The same is done for the temperature input.

The wide variability of sunlight in time and space adds further complexity to the optimization and control of the cultivation system (Pruvost et al., 2011). Both the lack and abundance of light will negatively influence the growth of the algae. The amount of irradiation from the sun that reaches the photobioreactor depends on the geographic location and the position of the reactor surface towards the sun. The position is influenced by the location of the reactor on earth (latitude and longitude), the earth's movement around the sun (differs during the year), and the earth's rotation around its own axis (diurnal cycle; hour-to-hour, minute-to-minute) (Slegers et al., 2013b). As an example, the average daily irradiance in the month of July in Amsterdam (the Netherlands) is 345 W/m^2. When comparing this to the month December in the same location, this is only 133 W/m^2. The location matters, as the average daily irradiance in July in Almeria (Spain) is 524 W/m^2 and for the month December 478 W/m^2 (Database). Therefore, the two different locations included in this model are: Almeria, Spain (36°50'25"N 2°28'05"W) and Amsterdam, the Netherlands (52°22'N 4°54'E).

The movement of the earth accounts for the climatic differences in the seasons. The following seasons are taken into account: spring, summer and fall. The meteorological calendar indicates that spring starts on the 1st of March and continues until the 31st of May. For the rest of the seasons, the meteorological calendar is used. Between the seasons, the day length as well as the light irradiation varies, which is also taken into account. For the information gathered by the meteorological station, see Appendix D. The following scenarios were made, where the temperature and the light intensity where combined per season per location.

Table 2-1: Seasonal temperature and light intensity details for the different locations.

Location	Time sun rise	Time sun down	Temperature range	Light intensity	Season
Almeria	7:00	19:00	10 - 24 °C	0 – 500 W/m^2	Spring
Almeria	7:00	20:00	18 – 31 °C	0 - 600 W/m^2	Summer
Almeria	7:00	19:00	12 – 29 °C	0 - 450 W/m^2	Fall
Amsterdam	7:00	19:00	2 - 17 °C	0 - 300 W/m^2	Spring
Amsterdam	6:00	22:00	10 - 22 °C	0 - 350 W/m^2	Summer
Amsterdam	7:00	19:00	4 – 14 °C	0 - 250 W/m^2	Fall

The values in this table were applied as a sinus wave. Meaning that the starting value of the sinus wave is equal to the first number of the range, and the highest value the temperature or light intensity will reach is the second number of the range. The sinus wave will be zero for the light intensity before the 'time sun rise' and after 'time sun down'. For the temperature, this is the first value of the range. Calculation will take place for the duration of one day, the final time being 24 hours.

Irradiance in the closed photobioreactor is composed of two fractions; direct light and diffused light. Direct light is solar radiation, which reaches a surface under a specific angle of incidence without encountering any obstacles in the atmosphere. Diffused light is light that has been scattered by the atmosphere and light reflected from other objects before falling on the surface from a variety of directions. These obstructions are often caused by clouds. In an ideal situation, temperature and irradiance would be investigated separately, to see what their individual effect is on the optimal temperature input trajectory. However, there is a connection between them. For example, cold days often have an overcast, while on warm days this is correlated with a clear sky. In addition, days in different seasons do not have the same daylight length; a sunny day in winter can have less total light than a cloudy day in summer.

2.7.2 Variation during a day

Noise will be added to the sinus wave to represent the cloud coverage. This will only be done for the light intensity, because this is affected the most by could coverage. To see the individual effect of cloud coverage on light and temperature cold and warm days are create. The following scenarios are used are described in the Table 2-2 below.

Table 2-2: Amount of noise added on the seasonal temperature and light intensity

Number of scenario	Type of day	Season	Temperature	Noise	Location
7	Cold	Spring	2 - 8 °C	5 %	Amsterdam
8	Cold	Spring	2 - 8 °C	10 %	Amsterdam
9	Warm	Spring	8 - 17 °C	5 %	Amsterdam
10	warm	Spring	8 - 17 °C	10 %	Amsterdam

For the location Amsterdam and the season spring, the day length and light intensity will be used out of Table 2-1. Table 2-2 will give the temperature range and the percentage noise that will be applied on the light intensity. The percentage noise tries to represent a day more realistic. The percentage noise illustrates the cloud cover, which is expressed in percentage of maximum cloud cover. The day length from Table 2-1 is based on Slegers et al. (2013b) and the light intensity on the Database of the European Commission.

3 Results & Discussion

In this research, different ambient temperatures and light intensities were applied to investigate the effect on the optimal input trajectory. This chapter presents the results of these optimal input trajectories. The different scenarios that are used are described in subchapter 0. Firstly an uncontrolled system simulation is given, after this optimal control is applied with Tomlab and finally piecewise linear trajectories. The latter is used to apply the scenarios with, which start with differences between locations and seasons and then variation during a day

3.1 Uncontrolled system simulation

A simulation was completed to get an impression what the temperature range would be and how the microalgae would respond to the temperature changes during the day. In this simulation, the control input is left out. The disturbance inputs are set on 10-20 °C (temperature range) and with a light intensity of 400 W/m^2, together with a time sun rise (TSR) on 6:00 and time sun down (TSD) at 18:00. The change in temperature and biomass concentration in the tubes (left) and in the bubble column (right) over one day is shown in Figure 3-1.

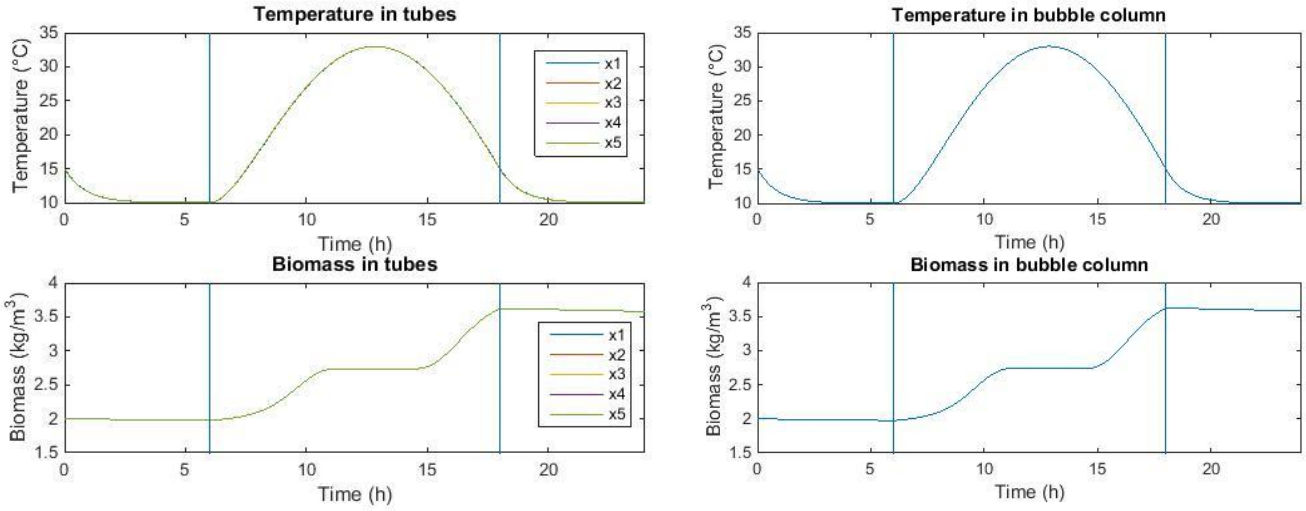

Figure 3-1: Temperature change and biomass concentration in tubes (left) and in the bubble column (right), without control input, simulated over one day, with the disturbance inputs being temperature range of 10-20 °C and a light intensity of 400 W/m^2 together with TSR at 6:00 and TSD at 18:00 (indicate by the vertical lines).

In this Figure 3-1, there is no substantial difference between the tubes and bubble column. This is caused by the fact that the start values of the tubes and the bubble column are the same and the volume is approximately the equivalent. Therefore, the amount of heat gained through the light intensity and the ambient temperature are nearly similar. Resulting in no visible difference between the temperature trajectory in the tubes and the bubble column. What stands out in both figures is that at the beginning the temperature moves down from 15 °C to the lower limit of 10 °C, indicating that the start value of the temperature are chosen higher than the ambient temperature causing the system to cool down. After TSR, the temperature increases from 15 °C to 33 °C. During the middle of the day, the temperature is at its highest, which is expected due to the outdoor circumstances. After TSD, the temperature moves down and becomes equal to the ambient temperature.

To conclude, a temperature profile of 15-33 °C is visible, with the temperature in the photobioreactor responding to the ambient temperature.

The microalgae *T. pseudonana* has an optimal temperature of 24.73 °C (Slegers et al., 2013b),the temperature in the tubes and the bubble column is above this temperature for a certain amount of time (as visible in Figure 3-1) during the day. This time is in the middle of the day, which corresponds with the fact that the sun is at its highest position during the middle of the day, supplying the most heat.
Next to a certain temperature, microalgae also need light to grow. This light intensity is only supplied after TSR. The lack of light is observable (in Figure 3-1, below), by the slightly declining line at the beginning and at the end of the biomass concentration graph. This decline can be explained by the fact that the respiration rate is higher than the specific growth rate. When there is light, the microalgae grow until the temperature in the culture is above the lethal temperature, which for this species of microalgae is 31.4 °C (Slegers et al., 2013b). The biomass concentration has a constant value in the middle of the day, indicating that the production stopped because the lethal temperature is reached. The total biomass growth on one day with the disturbance inputs as chosen show an increase of 1.6 kg/m^3. This corresponds with values found in literature. Chisti (2007) for example reported a volumetric productivity equal to 1.535 kg/m^3 per day for a photobioreactor. However, Jorquera et al. (2010) gives a volumetric productivity of 0.56 kg/m^3 per day for tubular photobioreactors. A work by Münkel et al. (2013) indicates that volumetric productivities equal to 1.25 kg/m^3 per day have been reached. All these studies use the same microalgae (*T. pseudonana*) as is used in this research. The difference in biomass growth can be explained by the different operating temperature and light intensity and the difference in photobioreactor types (Marsullo et al., 2015).

In sum, the temperature profile corresponds with the ambient temperature and the influence of the start values of the temperature is visible. The temperature gives a microalgae production that corresponds with value found in literature for this type of reactor and microalgae species. Nevertheless, the temperature reaches lethal temperature for a certain amount of hours during the day, which shows room for improvement in this case cooling.

3.2 Tomlab

Optimal control is applied with Tomlab, which is a modelling platform for solving applied optimization problems. The model was build, as described in the previous chapters. For Tomlab, the same conditions as in the uncontrolled system simulation were applied. In the following Figure 3-2 and Figure 3-3 the results of the applying optimal control with Tomlab is shown.

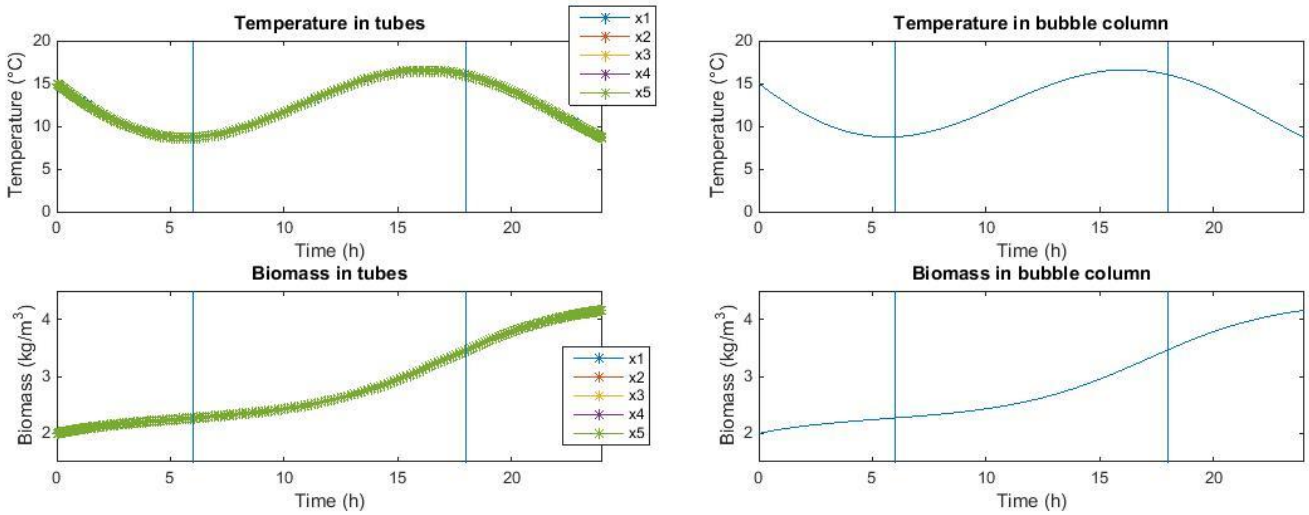

Figure 3-2: Temperature change and biomass concentration in tubes (left) and in the bubble column (right), with control input, simulated by Tomlab over one day, with the disturbance inputs being temperature range of 10-20 °C and a light intensity of 400 W/m² together with TSR at 6:00 and TSD at 18:00(indicate by the vertical lines).

In Figure 3-2, the temperature profile shows similar as in the simulation that it moves away from the start values until the ambient temperature and only after TSR it start heating up. Prominent is that the highest point of the temperature is not around the middle of the day (12:00), but later during the day (15:00). The maximal temperature in the tubes and the bubble column is around 15 °C. Therefore, the assumption can be made that the cooler is active, because known is that with the simulation, the maximum temperature becomes 33 °C.
To conclude, a temperature profile moves down from the initial condition (15 °C) to the ambient temperature (10 °C) and moves up. However, instead of reaching the maximal temperature 33 °C it remains around 15 °C and later moves back to the ambient temperature.

When comparing the simulation with the temperature profile that Tomlab gives the expectation is that, the cooler is on at the middle of the day. However, as seen in Figure 3-3 (which gives the heater and cooler trajectory), it is clear that the both of them are constant zero during the entire day. The start value for the heater was equal to $3 \cdot 10^3$ and for the cooler the start value was equal to zero. The result can be explained when the initial conditions are already quite profitable. However, even when changing the start values for both the heater and cooler or for the temperature and biomass concentration the same results of the control input trajectory is seen (Appendix E). Another problem occurs when looking at the gradient profile of the temperature for the tubes and the bubble column. Even though the control input is equal to zero the entire run, the temperature shows a pattern where influence of a control input is visible.

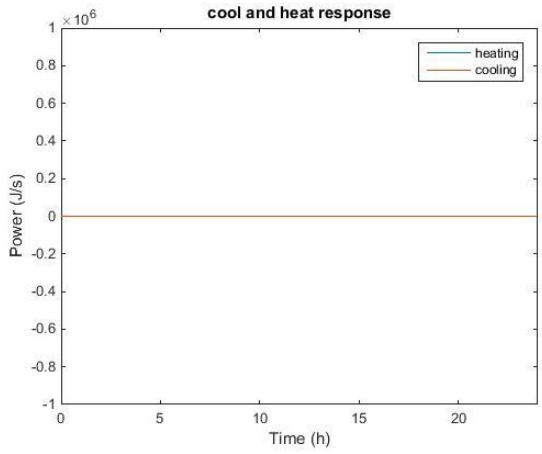

Figure 3-3: Control input trajectory of Tomlab for the reference system

The notification given by Tomlab is that optimal conditions are satisfied, and the cost function has a return value of € 51,59. The cost function took the revenue of the microalgae minus heating and cooling costs, with the microalgae production being around 2 kg/m^3 and a price of 25 €/kg and no heating and cooling, the returned value of cost function value seems logical. The sum(constr) has a value of 0.000006, which indicates that the optimal condition, which is reached, can be assumed to be valid.

The microalgae response to the temperature change that is given in Figure 3-2. The production is more than seen in the simulation, because the temperature stays below the lethal temperature. However, this temperature profile is not preferable even though it gives a higher biomass concentration because it does not reach the optimal temperature.

The code corresponding to this run can be found in Appendix F. The other run with different start values can be found in Appendix E. These results show that even with different start values the control input according to Tomlab should be equal to zero the entire time. The temperature presented does not correspond with the influence of the control input. The start values for the temperature are higher, expecting more cooling and less heating to be needed. However, the same results are shown. The temperature profile is similar to what was shown above. The same downwards and upwards movements are visible.

The assumption that the outcome of Tomlab maybe a local minimum is not plausible after two results both showing unrealistic values. Taking into account the high amount of collocation points (32*8) the expectation was that the system would come up with a fitted control input. But due to the long computation time it took, it is plausible to say that in combination with the stiff system, Tomlab is not able to generate credible results. This may have to do with the fact that this systems objective exist out of two parts (one part which is maximized and the other part being minimized) and therefore is not formulated like a typical Tomlab control objective. A typical formulated control objective in Tomlab states that value of the system should become as close as possible to a reference value.

The conclusion is drawn that Tomlab is not the suitable application for this model, therefore the following subchapter will describe the next method tried, piecewise linear.

3.3 Piecewise linear trajectories

The other method that was applied is piecewise linear. The values of the reference system (temperature range 10-20°C, light intensity 400 Wm^{-2}, TSR 6:00 and TSD 18:00) were used to see if this method showed better result than the other control method Tomlab. This was the case, (results shown in Appendix G) therefore the scenarios (location and season) and scenarios (variation during a day) are applied with piecewise linear trajectories.

3.3.1 Results of location and seasons.

The first scenario is the spring in Almeria (Spain), with a temperature of 10 – 24 °C and light intensity of 500 W/m2 with TSR being 7:00 and TSD 19:00 indicated by the vertical lines. The horizontal line indicates the optimal temperature for the microalgae T. pseudonana. In Figure 3-4 Figure 3-4the results of the first scenario are shown. On the left the temperature change and biomass concentration in the tubes and on the right the control input trajectory for this scenario. The graph for the bubble column can be found in the Appendix H-Scenario 1. The value of the cost function will be presented later on in Table 3-1

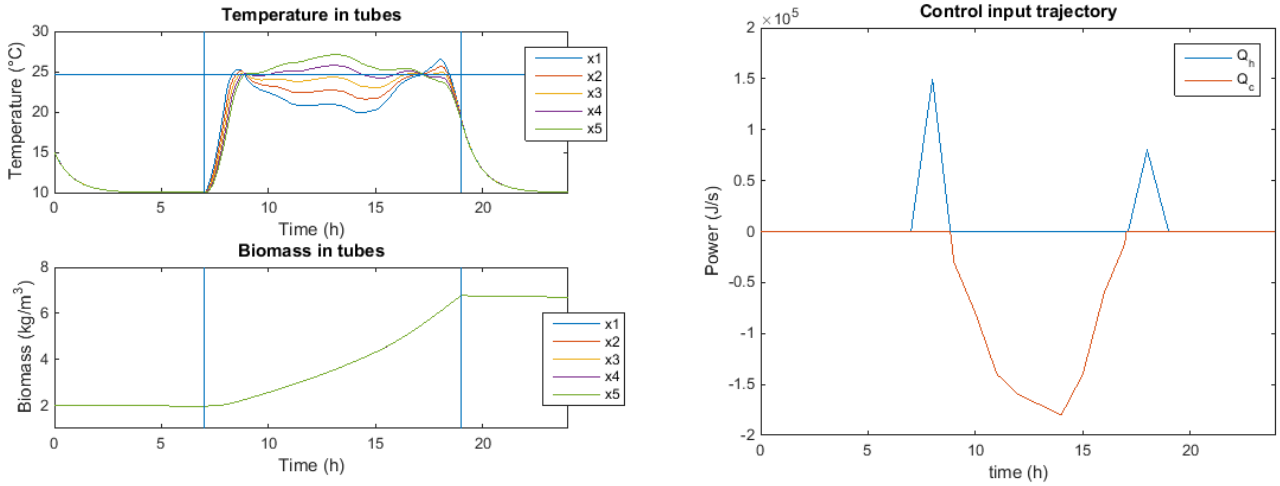

Figure 3-4: Temperature change and biomass concentration in the tubes (left) and the control input trajectory (right) simulated with piecewise linear trajectories for one day with the disturbance inputs of scenario 1

The results here shows are similar to the results of the uncontrolled system simulation, the temperature in the photobioreactor moves back to the ambient temperature before TSR and after TSD. There is a high peak needed to get the temperature of the system equal to the optimal temperature. When the ambient temperature starts to increase, the cooling starts. It moves down again, when the ambient temperature cools down. There is a peak in near the end, this to keep the temperature optimal until light not available anymore to make optimal usage of the light.

The second scenario was the summer in Almeria (Spain), with a temperature of 18 – 31 °C and light intensity of 600 W/m^2 with TSR being 7:00 and TSD 20:00 indicated by the vertical lines. The horizontal line indicates the optimal temperature for the microalgae *T. pseudonana*. In Figure 3-5, the results of the second scenario are shown. On the left the temperature change and biomass concentration in the tubes and on the right the control input trajectory for this scenario. The graph for the bubble column can be found in the Appendix H-Scenario 2. The value of the cost function will be presented later on in Table 3-1.

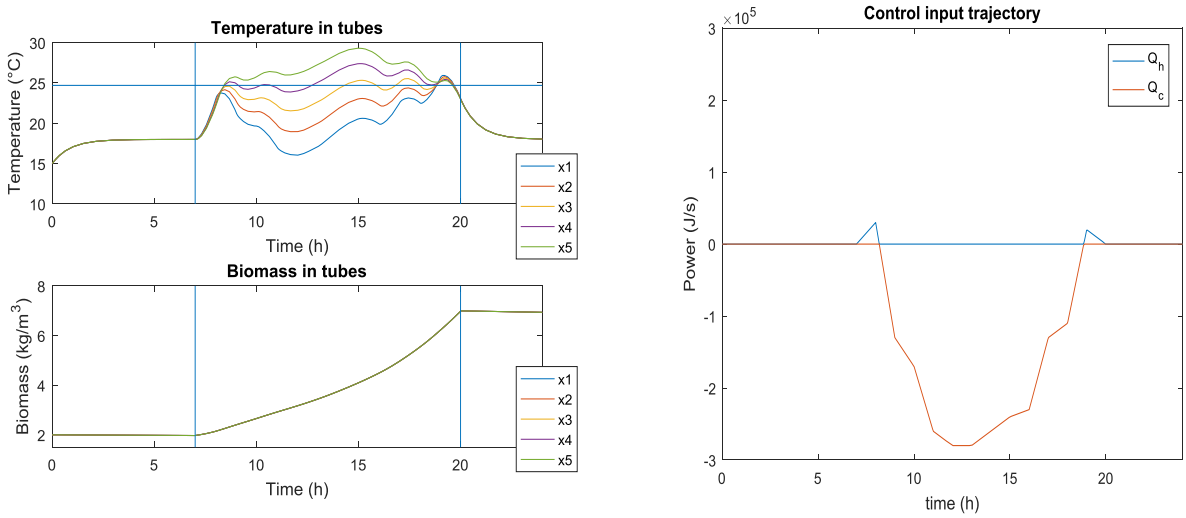

Figure 3-5: Temperature change and biomass concentration in the tubes (left) and the control input trajectory (right) simulated with piecewise linear trajectories for one day with the disturbance inputs of scenario 2

In this scenario, the ambient temperature is higher than the start values of the temperature in the system, which results in the temperature rise from 15 to 18 °C. Due to the fact that the ambient temperature is this high, the heating peak at the beginning of the day is less compared to previous figure (Figure 3-4). The different parts of the tubes are quite far apart from each other, the heating of the tubes causes this. The day length of this scenario is increased making light longer available which results in more biomass production.

The last scenario for the location Almeria (Spain) was the season fall, with a temperature of 12 – 29 °C and light intensity of 450 W/m^2 with TSR being 7:00 and TSD 19:00 indicated by the vertical lines. The horizontal line indicates the optimal temperature for the microalgae *T. pseudonana*. In Figure 3-6 the results of the third scenario are shown. On the left the temperature change and biomass concentration in the tubes and on the right the control input trajectory for this scenario. The graph for the bubble column can be found in the Appendix H-Scenario 3. The value of the cost function will be presented later on in Table 3-1.

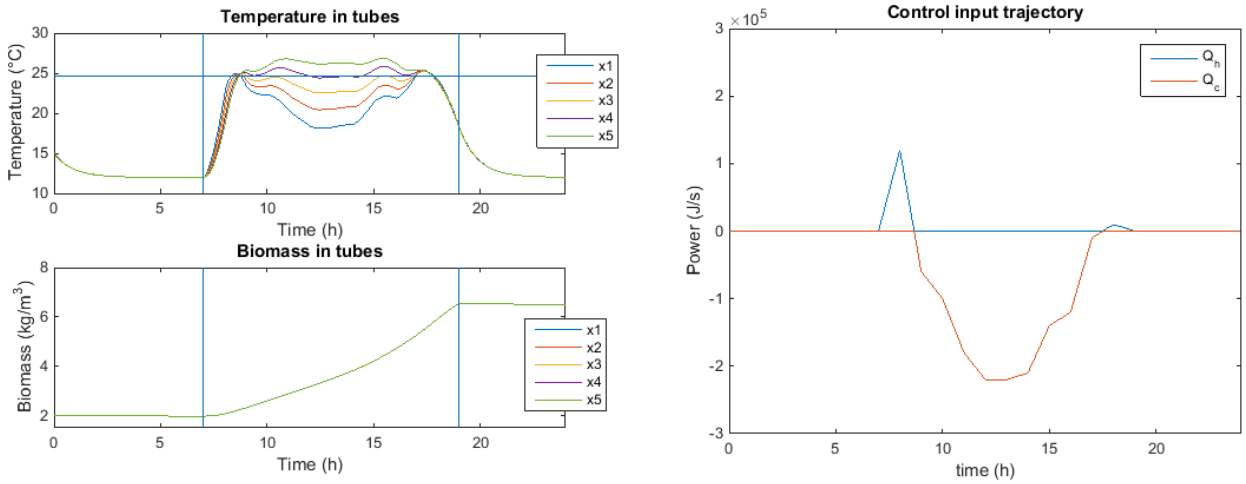

Figure 3-6: Temperature change and biomass concentration in the tubes (left) and the control input trajectory (right) simulated with piecewise linear trajectories for one day with the disturbance inputs of scenario 3

The control input trajectory for the fall shows a similar pattern when compare to the control input trajectory for the spring. Heating start after TSR with a large peak to reach optimal temperature and then when the ambient temperature starts moving up the control input starts cooling. What stands out in this figure is the difference between the peaks at the beginning of the day and at the end.

The previous figures (Figure 3-4 until Figure 3-6) showed the results of the location Almeria (Spain), the next figures show the results for the location Amsterdam (the Netherlands). The same seasons will be presented starting with spring, summer and fall.

In this scenario, the spring in Amsterdam (the Netherlands) is simulated, with a temperature of 2 – 17 °C and light intensity of 300 W/m^2 with TSR being 7:00 and TSD 19:00 indicated by the vertical lines. The horizontal line indicates the optimal temperature for the microalgae *T. pseudonana*. In Figure 3-7, the results of the fourth scenario are shown. On the left the temperature change and biomass concentration in the tubes and on the right the control input trajectory for this scenario. The graph for the bubble column can be found in the Appendix H-Scenario 4. The value of the cost function will be presented later on in Table 3-1.

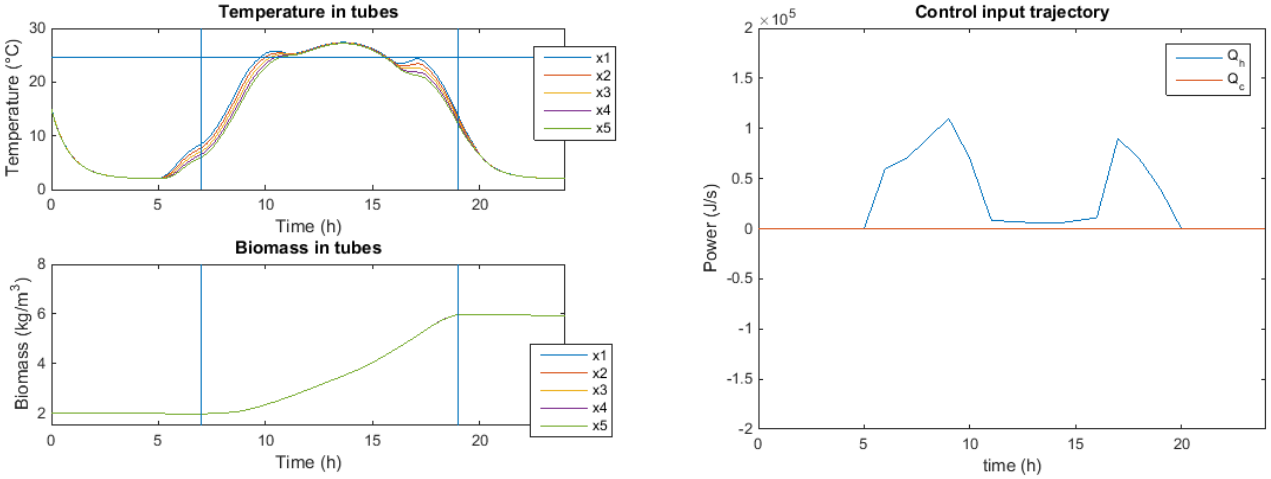

Figure 3-7: Temperature change and biomass concentration in the tubes (left) and the control input trajectory (right) simulated with piecewise linear trajectories for one day with the disturbance inputs of scenario 4

In this scenario is the ambient temperature here is 2 °C until 17 °C, which explains why there is no need for cooling. Due to the low ambient temperature, the heating starts earlier than seen before in the location Spain. The temperature profile shown here is moves away from the optimal temperature and shows a sine wave before reaching optimal temperature again. When comparing this scenario to the spring in Almeria, the temperature profile of the tubes show a more similar pattern to each other than in Spain.

This scenario is the summer in Amsterdam (the Netherlands), with a temperature of 10 – 22 °C and light intensity of 350 W/m^2 with TSR being 6:00 and TSD 22:00 indicated by the vertical lines. The horizontal line indicates the optimal temperature for the microalgae *T.* pseudonana. In Figure 3-8 the results of the fifth scenario are shown. On the left the temperature change and biomass concentration in the tubes and on the right the control input trajectory for this scenario. The graph for the bubble column can be found in the Appendix H-Scenario 5. The value of the cost function will be presented later on in Table 3-1.

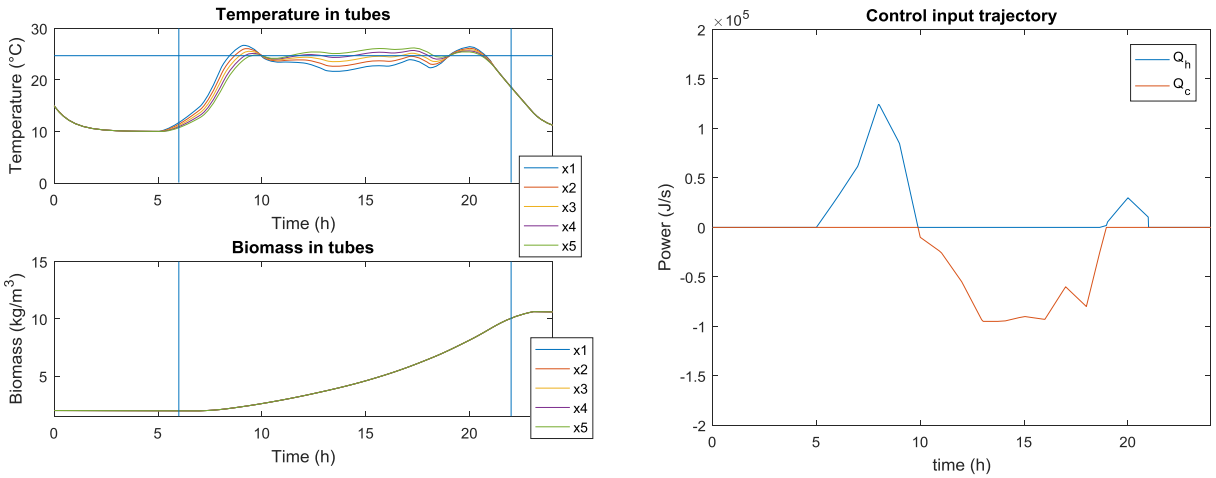

Figure 3-8: Temperature change and biomass concentration in the tubes (left) and the control input trajectory (right) simulated with piecewise linear trajectories for one day with the disturbance inputs of scenario 5

In this scenario, the ambient temperature is from 10-22 °C, which requires less time to heating the system up to the optimal temperature. When looking at the ambient temperature the expectation is that cooling is not necessary, however the light intensity also heats up the photobioreactor making cooling required. In this scenario, the day length is 3 hours more than the other scenario, making it possible to produce more biomass. This results in a microalgae concentration above 10 kg/m^3 compared to the value around 6 kg/m^3 in previous scenarios. The optimal temperature is reached almost the entire time between TSR and TSD. In this scenario the microalgae production continues to growth after TSD, but this growth is small.

This is the last scenario for location and seasons, the fall in Amsterdam (the Netherlands), with a temperature of 4 - 14 °C and light intensity of 250 W/m^2 with TSR being 7:00 and TSD 19:00 indicated by the vertical lines. The horizontal line indicates the optimal temperature for the microalgae. In Figure 3-9Figure 3-9, the results of the sixth scenario are shown. On the left the temperature change and biomass concentration in the tubes and on the right the control input trajectory for this scenario. The graph for the bubble column can be found in the Appendix H-Scenario 6. The value of the cost function will be presented later on in Table 3-1.

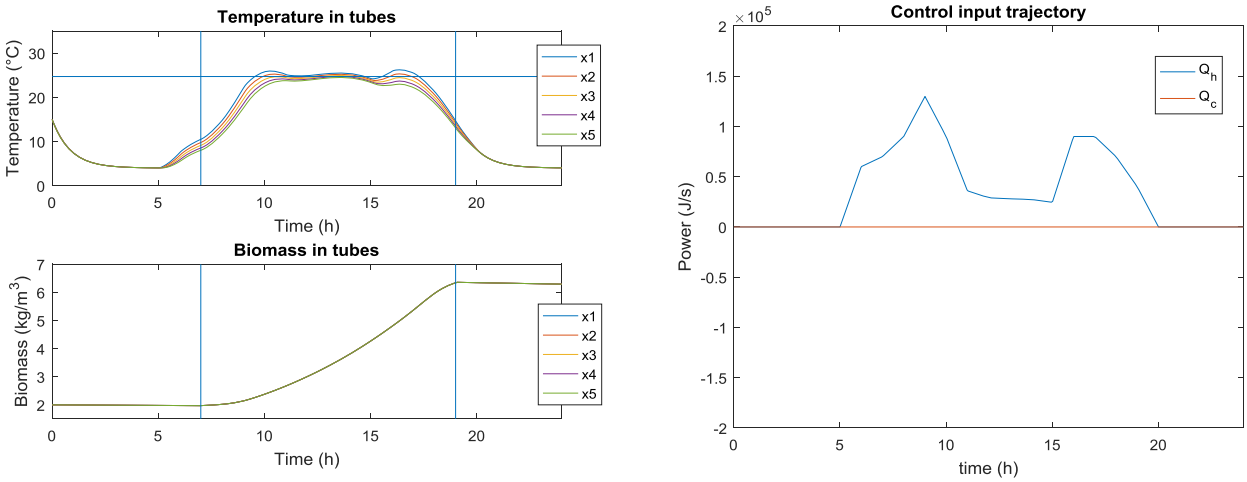

Figure 3-9: Temperature change and biomass concentration in the tubes (left) and the control input trajectory (right) simulated with piecewise linear trajectories for one day with the disturbance inputs of scenario 6

In this scenario, heating of the system similar in the other seasons of this location starts before TSR. However, it takes the system a while to reach the optimal temperature, when comparing to the location Spain. The ambient temperature indicates that only heating is required. The control input trajectory shown here resembles the control input trajectory of the fall in the same location.

In the table below (Table 3-1), all the values of the revenue of the microalgae and the cost for heating and cooling are given for all the six different scenarios run.

Table 3-1: Results of the cost function of the different scenarios applied for the locations and seasons.

Scenario number		**1**	**2**	**3**	**4**	**5**	**6**
Temperature trajectory		10 - 24 °C	18-31 °C	12-26 °C	2-17°C	10-22 °C	4-14°C
Light intensity trajectory		0-500 W/m^2	0-600 W/m^2	0-450 W/m^2	0-250 W/m^2	0-350 W/m^2	0-300 W/m^2
Time sun rise		7:00	7:00	7:00	7:00	6:00	7:00
Time sun down		19:00	20:00	19:00	19:00	22:00	19:00
Start values at t_0	T_{tubes}	15 °C	15 °C	15 °C	15 °C	15 °C	15 °C
	$C_{x_{tubes}}$	2 kg/m^3	2 kg/m^3	2 kg/m^3	2 kg/m^3	2 kg/m^3	2 kg/m^3
	T_{bubble}	15 °C	15 °C	15 °C	15 °C	15 °C	15 °C
	$C_{x_{tubes}}$	2 kg/m^3	2 kg/m^3	2 kg/m^3	2 kg/m^3	2 kg/m^3	2 kg/m^3
Revenue microalgae		€ 99.32	€ 104.31	€ 94.80	€ 82.95	€ 181.93	€ 90.70
Cost power		€ 34.48	€ 53.21	€ 36.31	€ 32.27	€ 31.66	€ 43.74
Cost function J		**€ 64.80**	**€ 51.10**	**€ 58.49**	**€ 50.68**	**€ 150.27**	**€ 46.95**

The microalgae biomass production differs from the lowest value in spring in the Netherlands to the highest value in the summer in the Netherlands. The microalgae revenue for summer in the Netherlands stands out with it being 2.2 times larger than the lowest microalgae revenue, which is the same location. When it comes to the cost for cooling and heating, the lowest value is in spring in the Netherlands, while the highest value in summer in Spain. Which is as expected, the hypothesis was that the summer in Spain could give the highest cost for cooling and heating. The spring in Spain, fall in Spain, spring in the Netherlands and summer in the Netherlands, are around the same range of cost for heating and cooling. The fall in the Netherlands has lower ambient temperatures requiring more heating. The revenue of the microalgae and the cost for heating and cooling result in the profit or cost function. The main profit can be seen in the summer in the Netherlands, this is mainly due to the high biomass production, which is causes by the larger day length. The lowest profit is for the season fall in the Netherlands, which is caused by the fact that the biomass production is quite low and the cost for this are relatively high.

3.3.2 Results variation during a day

The last scenarios were run to see how the system would responded to noise applied on the light intensity. The scenarios exist out of warm and cold days with 5% and 10% noise. The details of the scenarios are shown in Table 2-2. The results of this section is that it was almost impossible to find a start value where the cost function did not give an outcome equal to NaN (which means that the value is not recognized as a valid number). For example, when an optimal control input trajectory was found and saved but when later was tried to plot these results with the same values Matlab indicated that the cost function was equal to NaN. Therefore, no reliable results can be presented.

3.3.3 General discussion points

In previous sections, the results of this research were presented. In this part, the research the general discussion points are described. For the disturbance values only the ambient temperature and light intensity were taken into account. Only location, season and variation during a day were used, which was represented by a sine wave but therefore only taken direct sunlight into account. While scattered, indirect and ground reflection should be something to be considered because it will give more light and create more preferable situations (Chen et al., 2011; Slegers et al., 2013b).

In the following figure, the growth rate depending on the temperature is presented, to see how the growth rate changes when moving away from the optimal temperature.

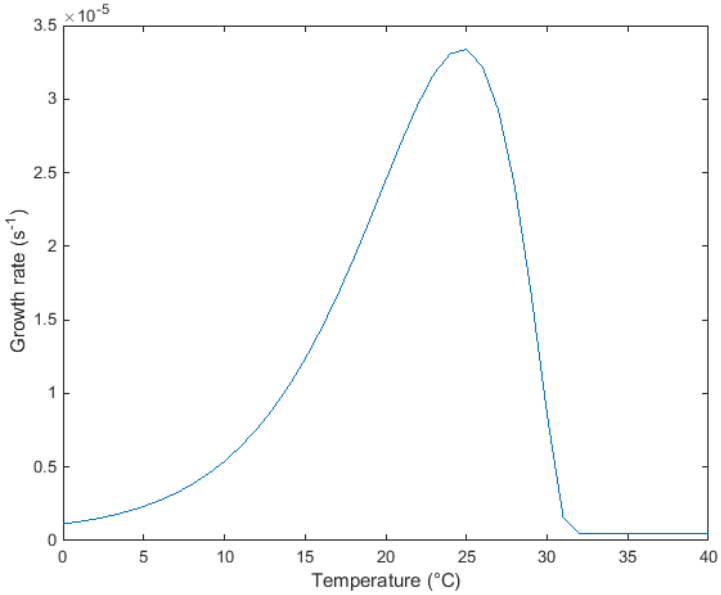

Figure 3-10: The growth rate (s^{-1}) as a function of the Temperature (°C) for *T. pseudonana*

In Figure 3-10 is visible that the growth rate decreases when you are slightly above the optimal temperature. In the graphs (Figure 3-4 until Figure 3-9) presented, most of the time the first and/or second part of the tube are above the optimal temperature and the remaining parts of the tubes is below. In this figure, it is visible that between the temperature of 20-25 °C, the growth rate increases from $2.4 \cdot 10^{-5}$ (s^{-1}) to $3.3 \cdot 10^{-5}$ (s^{-1}), while from 25-30 °C the growth rate decreases from $3.3 \cdot 10^{-5}$ (s^{-1}) until $8.5 \cdot 10^{-6}$ (s^{-1}). The results of this figure indicate that is it better to have values slightly lower than the optimal temperature compared to higher than the optimal temperature.

Next to the sensitivity of the temperature, there are two different light effects that need to be taken into account; light-inhibition and Lambert–Beer in opaque solutions. In the applied scenarios, the light intensity ranges from 250-600 W/m^2 which corresponds to 491-1176 $\mu mol/m^2 s$. In Figure 3-11 is shown what the microalgae *T. pseudonana* growth rate is in standard conditions compared to when subjected to photo–inhibition. This figure shows that the growth rate decreases after a photon flux density lower than 250 $\mu mol/m^2 s$. In this research, there was no correction done for photo-inhibition making this effect visible in the seasons where the light intensity is larger. In the figure, the blue lines indicate the light intensity for the location the Netherlands and the red lines for Spain. This shows that the growth rate in Spain was lower compared to the Netherlands. Photo-inhibition is the explanation why in the Netherlands better results with regards to the microalgae production were seen compared to Spain. The microalgae revenue could be improved when the light intensity would be reduced.

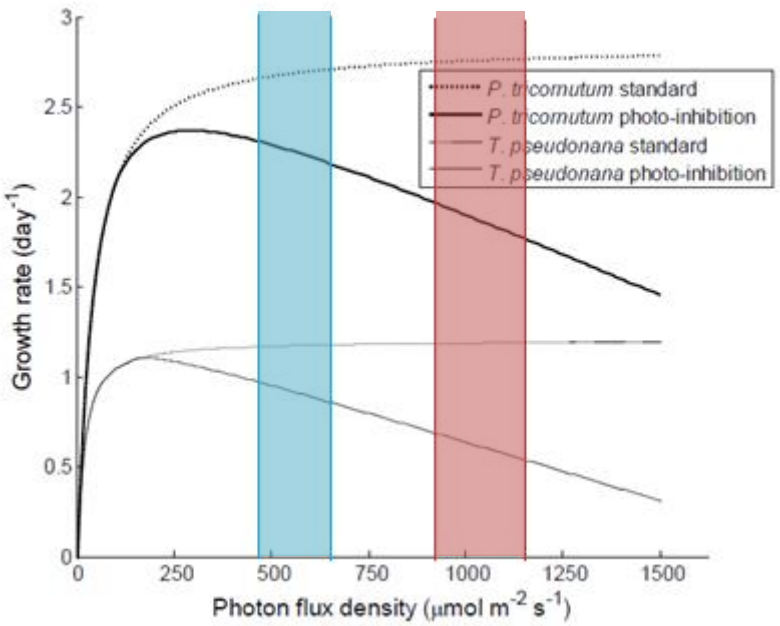

Figure 3-11: Specific growth rate (day^{-1}) with and without photo-inhibition (from Slegers et al. (2013b)) with the blue lines being the minimum and maximum light intensity of Amsterdam and the red lines being the minimum and maximum light intensity of Almeria.

Besides light-inhibition, there was another effect visible when looking at the results. In every graph of the scenarios (Figure 3-4 until Figure 3-9) the values directly after TSR and before TSD show a similar pattern. The temperature moves straight up and the microalgae concentration is level for a short while. This can be contributed to the light intensity, as shown in the Figure 3-12. The light intensity is zero before TSR and start moving up when TSR is passed making light come in later.

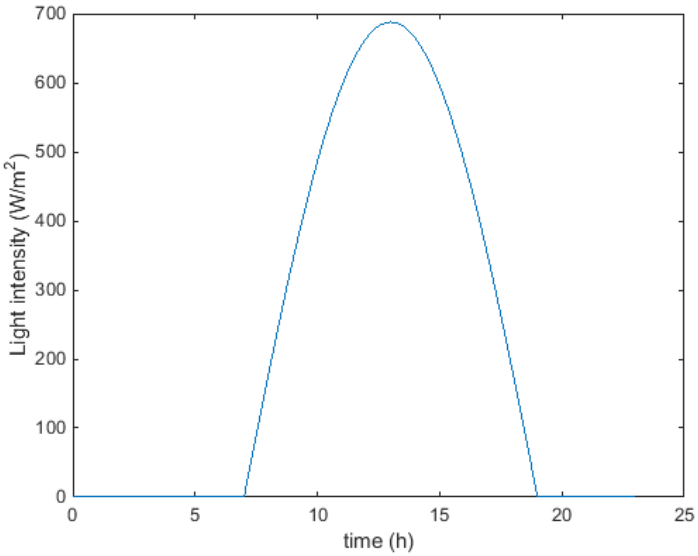

Figure 3-12: Light intensity (W/m^2) during one day with TSR 7:00 and TSD 19:00

In Figure 3-11 is shown that low light intensity has a high growth rate but still a level microalgae concentration is seen in the results (Figure 3-4 until Figure 3-9) at the beginning and end of the day. This is due to the fact that at the beginning of the day the microalgae cells are a small amount. A high

growth rate does not have an added value at that moment because the microalgae cells are low. This phenomenon explains the level microalgae concentration at the beginning of the day, for the end of the day there is another explanation possible, namely opaque. In this system, Lambert – Beer equation is taken into account, meaning that for the relationship between absorbance and concentration of the microalgae is adjusted. Nevertheless, opaque will still occur with this high amount of microalgae biomass concentration, which results in a level biomass concentration just before TSR. This can also be due to the fact that with optimal control it is known that right before final time, the results are not considered to be that important and the results are not always desired.

As seen in this research, the most profit can be made in the Netherlands. However, the price of the harvest microalgae has a direct correlation to this profit. For example, if the price would decrease from 25 €/kg to 5 €/kg, no positive profit would be shown. When it comes to the heater and cooler, in this research there efficiency is equal, but the cost for the heater are double compared to the cooler. In this research the thermal energy costs are calculated for one day, showing promise for the location the Netherlands over the location Spain. However, Ruiz et al. (2016) shows potential for Spain by calculating the microalgae production (cultivation and harvesting) cost (€/kg) for the same type of photobioreactor to be equal to 8.9 €/kg in the Netherlands and 5.2 €/kg in Spain. In general, it is tough that Spain is the better location to production microalgae. However, the species of microalgae that is used in this research is known to have a relative slow growth rate compare to other microalgae. The optimal temperature of the microalgae is 24.74 °C (Slegers et al., 2013b). When looking at the ambient temperature of both locations, it can been seen that the average temperature in the Netherlands lays closer to the optimal temperature, therefore already creating a preference for the location the Netherlands compared to the location Spain.

When it comes to the methods used, Tomlab is known to be suitable for solving optimal control problems, but the result of the control input trajectory was an unreliable result. The outcome of Tomlab that is given for the cost function is similar when comparing to the outcome of the cost functions of piecewise linear trajectories. However, the optimal control input trajectory not, indicating that there may be a mistake when generating the figures of Tomlab. Piecewise linear trajectories has a large amount of intervals, due to this high amount the higher the chance there is to get stuck in a local minimum. Another problem for this method was to find good starting values for the control input. The starting values determine which local minimum the result presents. The temperature profile is close to the optimal temperature however, this mainly depends on the initial guess given the system and will give a local minimum based on the initial guess.

By only taken into account the temperature as a control factor, the system becomes dependent on a single control factor, whereby a slight change will influence the entire system. At this moment, it is assumed that the biomass in the reactor will be the same level at the beginning of each day so that the same control can be applied every day. Thus assuming that harvesting takes place each day at the end of the day, and the amount that is harvest is the final concentration until the start value. A lot of research has been done on what type of harvesting is suitable for a certain system (Grognard et al., 2014). Next to this the preferable harvesting time is researched (Grognard et al., 2014), including the optimal adequate control method (Van Straten et al., 2010). Aforementioned studies show that it would be possible to time the moment of harvesting and the amount of harvesting to include also optimal harvesting. In the end, the main goal of this research was to find out if production cost could be reduced by the implication of optimal control on temperature. However, with cultivation of microalgae not only production has to be taken into account but harvest as well. Further research should be done to indicate what type of harvest is best suited, in this situation.

4 Conclusion

The research questions made in this research were described as follows: What is the optimal input trajectory for a standard situation? How is the optimal input trajectory affected by the season, location and variation during a day? And finally; is it possible to translate the optimal control strategies for different situations into heuristic control rules?

The mathematical analysis of the model showed that the model was a stiff system. The model was adapted by using pseudo-steady-state for the heater exchanger. The proposed software Tomlab, turned out not to be suitable for this system because the results shown were unreliable. Optimization of piecewise linear trajectories showed results with a positive monetary outcome and microalgae growth higher than the uncontrolled system simulation. The standard situation or also called reference system has a specific ambient temperature and light intensity. The first research question can be answered with the following figure (Figure 4-1) were the optimal input trajectory for a standard situation can be seen on the left.

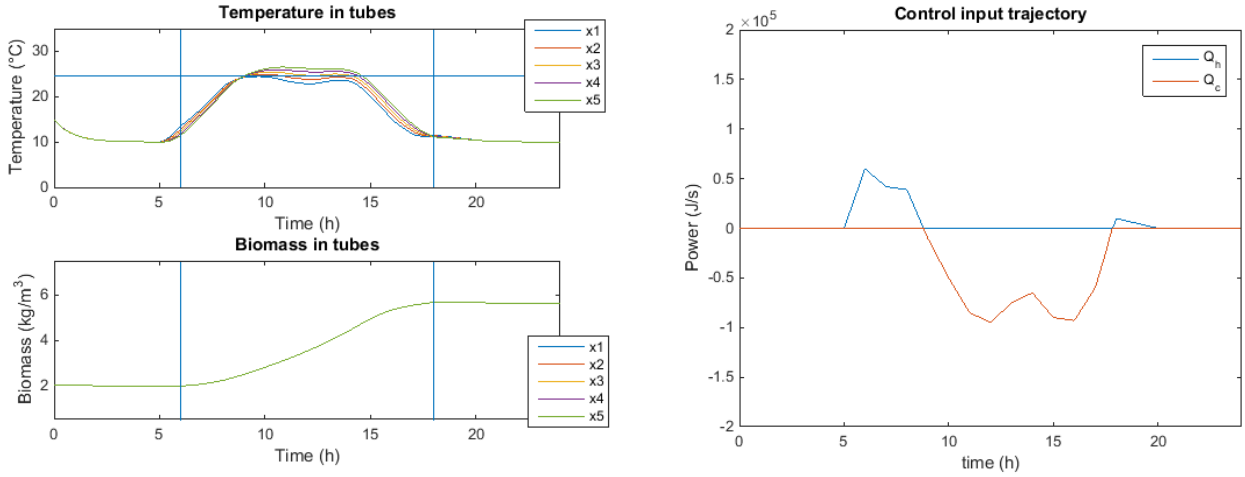

Figure 4-1: Temperature change and biomass concentration in the tubes (left) and the control input trajectory (right) for the piecewise linear trajectories reference system (temperature range of 10-20 °C, light intensity of 400 W/m², TSR being 6:00 and TSD 18:00).

The second research question asked was how the optimal control input trajectory was affected by location, seasons and variation during a day. In chapter 3.3.1 (location and season) and 3.3.2 (variation during a day) the results for the different scenarios are given.
All results have a strong peak at the beginning to get the ambient temperature until the optimal temperature, followed by cooling or heating depending on the ambient temperature. The days ends with a peak. In general, the same peaks are observable in all the control input trajectories but in different sizes and on different moments. The peaks depends per scenario on the light availability and ambient temperature. These results show that in both locations the control input trajectory for the season spring resembles the control input trajectory for the season fall. In the location the Netherlands, the heating starts earlier due to the colder outdoor conditions. However, even though heating starts earlier the optimal temperature is reached later in comparison to the location Spain. In Spain, photo-inhibition plays a role making the microalgae production less compared to the Netherlands.

In this research, with the price of microalgae being € 25/kg, cost of heating € 0.04/kWh and cost of cooling € 0.02/kWh, the cost function shows the highest profit for the summer in the Netherlands, namely € 150,27 per day. The costs for heating and cooling are approximately between € 31,- and € 54,- per day. The lowest profit of the six scenarios is also in the Netherlands, in the fall. All profits are positive indicating that with the price of microalgae and for heating and cooling taken in this case, it

is profitable for the microalgae production to keep the temperature in the photobioreactor at an optimal temperature.

The results presented in this research lead to the conclusion that the location and season have effect on the optimal input trajectory. The heuristic control rules that can be drawn from this research are as follows: during the night no heating or cooling is required, this has to do with the effect that respiration takes places and the cost of cooling and/or heating are too high. When light is available the temperature in the photobioreactor should be at the optimal temperature. It is known when light becomes available, making it possible to control the temperature in such way that the optimal temperature is reached at the right time. How much controlling of the temperature in the photobioreactor is needed depends on the ambient temperature. When the ambient temperature is relatively low, the heating should start earlier. The heating and/or cooling to keep the temperature at ambient temperature should continue when enough light is available. With the price of the microalgae as used in this research it is feasible to keep the temperature at optimal temperature when light is available. Price is an important factor, for the different scenarios a minimum price should be established to define whether to use optimization or not.

When it comes to the variation during a day, the conclusion can be made that with optimization of piecewise linear trajectories no reliable results will be given. The research question when it comes to how the optimal input trajectory is affected by variation during a day can therefore not be answered and no heuristic rule can be made.

5 Recommendations & Outlook

First recommendations will be done for the two main problems that the results show: variation during a day and the sensitivity when it comes to the initial guess. A recommendation will be made for these problems. Later an outlook will be given when it comes to the future of closed outdoor photobioreactors.

This system is based on data, which was represented by sine waves, which represents the main trend of outside data but this does not resemble realistic data. The noise that is applied trying to mimic variations during the day shows unreliable results. When using real data this may not occur therefore, real data should be used to see if a heuristic rule could be made for the variation during a day. When a heuristic rule is made, the recommendation is that this rule and together the heuristics rules when it comes to location and season should be validated with real data.

Another problem that occurred in this research, is the sensitivity of the initial guess for the optimization of piecewise linear trajectories. A recommendation would be to use less time intervals or using initial guesses, which resemble each other, so that the same optimal solution will be found each time.

When it comes to the systems prospect, the system is profitable in this research however, the applied price for microalgae may change in the future. In addition, with unknown prices of the future, the outlook will be that the microalgae production system will be coupled with another application to reduce costs and make microalgae more competitive for different industrial applications. This coupling should be made for the temperature and light intensity. This coupling with other applications can for example be with an application that already produces heat. Other examples of coupling are with combustion power plants or other CO_2 sources or use nutrients from wastewater treatment facilities or low quality water (Bernard, 2011; De la Hoz Siegler et al., 2012; Ugwu et al., 2008).

Next to temperature, the light should also be coupled or more regulated so that the optimal microalgae production could be reached. In this research photo-inhibition occurs, when light availability would be more regulated higher microalgae production can be reached. It is known, that the light of the sun varies with the weather, seasons and locations making the light intensity supply unstable. Artificial light would be a solution, however this is relatively expensive. A solution/combination is proposed by Chen et al. (2011). They recommend a light dependent resistor (LDR) for online monitoring of the irradiation intensity on the photobioreactor. The light intensity from the sun is used for daytime illumination. But, if the light intensity decreased below a certain set value (due to clouds/rainy days), an artificial light source (multi-LED light sources) are automatically activated. This ensures a continuous, sufficient and stable light supply for inside and outside the photobioreactor. It is important to remember that the microalgae do need a dark period in the production cycle, but this can be considered in the model. This combination limits the amount of electricity consumption needs compared to continuous artificial light. However, to further decrease electricity consumption, Chen et al. (2011) proposed to install also solar panels and a wind power generator. The solar panels are used to collect solar radiation from the sunlight, but because sunlight is not continuously, the wind power generator is used as additional complement. Together, the solar panels and wind power generator supply all the energy required by the multi-LED light sources. With this system the microalgae cultivation could take place with zero electricity consumption.

Finally, to make microalgae production really compatible in the industrial applications there needs to be a production on larger scale. However, when increasing production new constraints and problems will pop up (Ugoala et al., 2012).

References

Arthur E. Bryson, J. (1999). *Dynamic Optimization*.

Béchet, Q., Shilton, A., & Guieysse, B. (2013). Modeling the effects of light and temperature on algae growth: state of the art and critical assessment for productivity prediction during outdoor cultivation. *Biotechnology advances, 31*(8), 1648-1663.

Berenguel, M., Rodrıguez, F., Acién, F., & Garcıa, J. (2004). Model predictive control of pH in tubular photobioreactors. *Journal of Process Control, 14*(4), 377-387.

Bernard, O. (2011). Hurdles and challenges for modelling and control of microalgae for CO 2 mitigation and biofuel production. *Journal of Process Control, 21*(10), 1378-1389.

Chen, C.-Y., Yeh, K.-L., Aisyah, R., Lee, D.-J., & Chang, J.-S. (2011). Cultivation, photobioreactor design and harvesting of microalgae for biodiesel production: a critical review. *Bioresource technology, 102*(1), 71-81.

Chisti, Y. (2007). Biodiesel from microalgae. *Biotechnology advances, 25*(3), 294-306.

Database, E. C. Solar irradiance database Retrieved 4-4, 2018, from http://re.jrc.ec.europa.eu/pvg_tools/en/tools.html

De la Hoz Siegler, H., McCaffrey, W., Burrell, R., & Ben-Zvi, A. (2012). Optimization of microalgal productivity using an adaptive, non-linear model based strategy. *Bioresource technology, 104*, 537-546.

Fernández, I., Acién, F., Fernández, J., Guzmán, J., Magán, J., & Berenguel, M. (2012). Dynamic model of microalgal production in tubular photobioreactors. *Bioresource technology, 126*, 172-181.

Fernández, I., Acién, F. G., Berenguel, M., & Guzmán, J. L. (2014). First principles model of a tubular photobioreactor for microalgal production. *Industrial & Engineering Chemistry Research, 53*(27), 11121-11136.

Fernández, I., Peña, J., Guzman, J., Berenguel, M., & Acién, F. (2010). Modelling and control issues of pH in tubular photobioreactors. *IFAC Proceedings Volumes, 43*(6), 186-191.

Geider, R., MacIntyre, H., & Kana, T. (1997). Dynamic model of phytoplankton growth and acclimation: responses of the balanced growth rate and the chlorophyll a: carbon ratio to light, nutrient-limitation and temperature. *Marine Ecology Progress Series*, 187-200.

Grognard, F., Akhmetzhanov, A. R., & Bernard, O. (2014). Optimal strategies for biomass productivity maximization in a photobioreactor using natural light. *Automatica, 50*(2), 359-368.

Guterman, H., & Ben-Yaakov, S. (1990). On-line optimization of biotechnological processes: I. Application to open algal pond. *Biotechnology and Bioengineering, 35*(4), 417-426.

Hermanto, M. B. (2009). *Identification of algae growth kinetics* (Master thesis), Wageningen univeristy

Hu, D., Li, M., Zhou, R., & Sun, Y. (2012). Design and optimization of photo bioreactor for O 2 regulation and control by system dynamics and computer simulation. *Bioresource technology, 104*, 608-615.

Jorquera, O., Kiperstok, A., Sales, E. A., Embirucu, M., & Ghirardi, M. L. (2010). Comparative energy life-cycle analyses of microalgal biomass production in open ponds and photobioreactors. *Bioresource technology, 101*(4), 1406-1413.

Langhans, R. W., & Tibbitts, T. (1997). Plant growth chamber handbook.

Lee, E., Jalalizadeh, M., & Zhang, Q. (2015). Growth kinetic models for microalgae cultivation: a review. *Algal Research, 12*, 497-512.

Lösing, M. B. (2011). *Modelling & simulating microalgae production in an open pond reactor.* (Master thesis), Wageningen Univeristy

Malek, A., Zullo, L. C., & Daoutidis, P. (2015). Modeling and dynamic optimization of microalgae cultivation in outdoor open ponds. *Industrial & Engineering Chemistry Research, 55*(12), 3327-3337.

Marsullo, M., Mian, A., Ensinas, A. V., Manente, G., Lazzaretto, A., & Marechal, F. (2015). Dynamic modeling of the microalgae cultivation phase for energy production in open raceway ponds and flat panel photobioreactors. *Frontiers in Energy Research, 3*, 41.

Mata, T. M., Martins, A. A., & Caetano, N. S. (2010). Microalgae for biodiesel production and other applications: a review. *Renewable and Sustainable Energy Reviews, 14*(1), 217-232.

Mehlitz, T. H. (2009). Temperature influence and heat management requirements of microalgae cultivation in photobioreactors.

Mott, D. R., Oran, E. S., & van Leer, B. (2000). A quasi-steady-state solver for the stiff ordinary differential equations of reaction kinetics. *Journal of Computational physics, 164*(2), 407-428.

Pruvost, J., Cornet, J., Goetz, V., & Legrand, J. (2011). Modeling dynamic functioning of rectangular photobioreactors in solar conditions. *AIChE Journal, 57*(7), 1947-1960.

Quinn, J., De Winter, L., & Bradley, T. (2011). Microalgae bulk growth model with application to industrial scale systems. *Bioresource technology, 102*(8), 5083-5092.

Ras, M., Steyer, J.-P., & Bernard, O. (2013). Temperature effect on microalgae: a crucial factor for outdoor production. *Reviews in environmental science and bio/technology, 12*(2), 153-164.

Ruiz, J., Olivieri, G., de Vree, J., Bosma, R., Willems, P., Reith, J. H., . . . Barbosa, M. J. (2016). Towards industrial products from microalgae. *Energy & Environmental Science, 9*(10), 3036-3043.

Slegers, P., Wijffels, R., Van Straten, G., & Van Boxtel, A. (2011). Design scenarios for flat panel photobioreactors. *Applied energy, 88*(10), 3342-3353.

Slegers, P., Wijffels, R., Van Straten, G., & Van Boxtel, A. (2013a). Scenario analysis of large scale algae production in tubular photobioreactors. *Applied energy, 105*, 395-406.

Slegers, P., Wijffels, R., Van Straten, G., & Van Boxtel, A. (2013b). Scenario evaluation of open pond microalgae production. *Algal Research, 2*(4), 358-368.

Suh, I. S., & Lee, C.-G. (2003). Photobioreactor engineering: design and performance. *Biotechnology and Bioprocess Engineering, 8*(6), 313.

Svaldenis, A. (2014). Cultivating Algae in a Photobioreactor: CO2 fixation, synthetic wastewater nutrient removal and biomass production using the green algae species Chlorella pyrenoidosa.

Ugoala, E., Ndukwe, G., Mustapha, K., & Ayo, R. (2012). Constraints to large scale algae biomass production and utilization. *Journal of Algal Biomass Utilization, 3*(2), 14-32.

Ugwu, C., Aoyagi, H., & Uchiyama, H. (2008). Photobioreactors for mass cultivation of algae. *Bioresource technology, 99*(10), 4021-4028.

Van Boxtel, A. (2016). *Modelling of Biobased Production Systems*. [Course material]. Wageningen University

Van Straten, G., Slegers, P., Van Willigenburg, L., Bosma, R., Van Boxtel, A., & Wijffels, R. (2010). Toward optimal control of flat plate photobioreactors: the greenhouse analogy? *IFAC Proceedings Volumes, 43*(26), 299-303.

Van Willigenburg, L. (2017). *System and Control Theory*. [Course material]. Wageningen Univeristy.

Wang, B., Lan, C. Q., & Horsman, M. (2012). Closed photobioreactors for production of microalgal biomasses. *Biotechnology advances, 30*(4), 904-912.

Appendix

A. Growth kinetics

Microalgae have a different growth pattern than plants. Instead of increasing in size or weight, they enlarge in the number of single cells. As descripted, there are various factors that influences the microalgae growth. However, when this is not the case and the culture is a homogenous batch process, the growth kinetics of the microalgae can be determined. In this homogenous process, nutrient supply is limited and nothing is added or removed from the culture.

The microalgae growth goes through a couple of phases: lag phase, exponential phase, declining growth phase, stationary phases and death phase. In the first phase, the lag phase, the growth is delayed because it takes time for the culture to adjust to the new conditions. After the adjustment, the microalgae can/will start growing. This happens in the exponential phase, here the cells grow and divide as an exponential function of time. It is important to note that during this phase, neither light intensity nor nutrients are limiting factors for the growth. This is followed by cell division which slows down becomes light becomes limiting. This causes for an accumulation, which is constant. After this, an equilibrium is reached in the stationary phase. The growth is now approaching a limiting value (the maximum biomass concentration possible in this system). Processes like storage of carbon products take place. The last phase, the death phase, is caused by unfavourable conditions, for example depletion of nutrients, overheating, pH disturbance or contamination. In this phase the microalgae cell concentration declines rapidly.

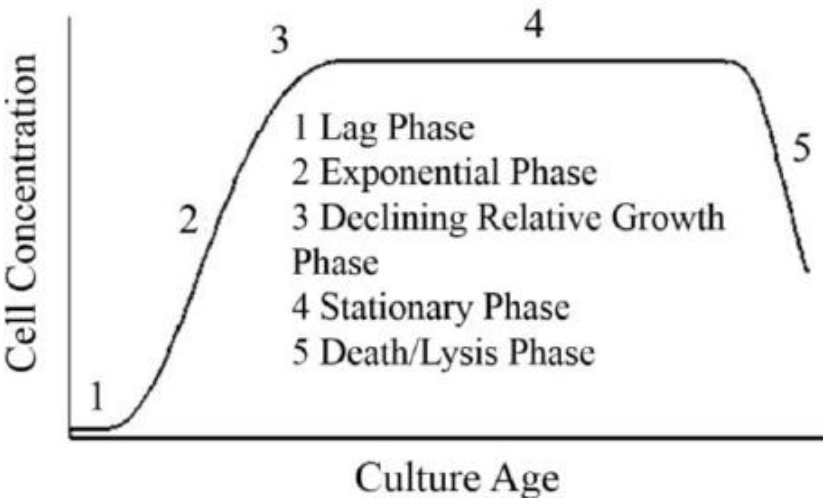

Figure A-1: The growth phases of microalgae cultures

All these phases are visible in Figure A-1, in practice the phases are not always as noticeable as shown in the Figure A-1. There are certain things that may be different, for example the slope may vary in magnitude, length or height. In addition, the transitions from one phase to another may be shaped differently. The actual shape of the microalgae growth phases is based on the inoculation material, the nutrient concentration, and the environmental conditions such as light intensity, temperature and pH (Lee et al., 2015; Mata et al., 2010; Mehlitz, 2009).

B. Model parameters summary

The following section presents an overview of the parameters of the model with the specific assumptions explained. Model inputs and parameters for photobioreactor are summarized in Table B-1 for the temperature model in Table B-2, the values for the light intensity in Table B-3 and for the microalgae growth biomass model in Table B-4.

In Table B-1, the values for the parameters of the photobioreactor are given. The values were based from the paper of Fernández et al. (2014) which gives a mathematical model for everything that happens in a photobioreactor.

Table B-1: The parameters value of the photobioreactor

Abbreviation	Value	Unit
C_p	4183	J kg^{-1} $°C^{-1}$
ρ	1000	kg m^{-3}
$length$	80	m
d_b	0.4	m
$height_{bubble}$	3.2	m

A couple of equations are here presented, which were all needed to in the end come up with the dilution rate. The two equation will calculate the volume in the tubes and the bubble column, while the formulas followed by these describe how to calculate the dilution rate.

$$V_{liq} = \pi \frac{1}{2} d_t^2 \, length \tag{B.1}$$

$$V_{bubble} = \pi \frac{1}{4} d_b^2 \, length \tag{B.2}$$

$$F = Q_{liq} \tag{B.3}$$

$$V_{liq} = \frac{V}{n} \tag{B.4}$$

$$D = \frac{F}{V} \tag{B.5}$$

Dilution rate is calculated, with the Q_{liq} of the temperature model. In the following table the parameters for the temperature model are given also based on the paper of Fernández et al. (2014).

Table B-2: The parameters value of the temperature model

Abbreviation	Value	Unit
α_t	0.9725	Dimensionless
d_t	0.084	m
a	0.5411	Dimensionless
h_t	30	J s^{-1} m^{-2} $°C^{-1}$
α_b	0.1052	Dimensionless
S_b	4.0212	m^2
h_b	11.186	J s^{-1} m^{-2} $°C^{-1}$

In table B-3 the value is given for the parameter of the lambert-Beer law.

Table B-3: Lambert-Beer law coefficient.

Abbreviation	Value	Unit	Reference
k_a	0.269	(m^2 kg^{-1})	(Quinn et al., 2011)

The following table will give the parameters of the biomass model, based on the paper of (Slegers et al., 2013b)

Table B-4: The parameters value of the biomass model

Abbreviation	Value	Unit
r_m	$5.79 \cdot 10^{-7}$	s^{-1}
T_{let}	31.40	°C
T_{opt}	24.73	°C
β_T	1.83	Dimensionless
α_{photo}	10	g C mol^{-1} photons m^2 g^{-1} Chl*a*
Θ_{max}	0.08	g^{-1} Chl*a* g^{-1} C
μ_{max}	$3.81 \cdot 10^{-7}$	s^{-1}

C. Nomenclature

Abbreviation	Description	Unit
a	Constant representing solar irradiance absorptivity	(-)
C_p	Volumetric heat capacity of growth medium	(J kg^{-1} °C^{-1})
C_x	Biomass concentration	(Kg m^{-3})
d	Vector of disturbance	(-)
D	Dilution rate over time	(s^{-1})
d_b	Diameter tubes	(m)
D_p	Tube diameter in p part	(m)
d_t	loop diameter of tubes	(m)
f_T	Temperature factor	(-)
$height_{bubble}$	Height of the bubble column	(m)
h_b	Heat transfer coefficient to ambient in bubble column	(J s^{-1} m^{-2}°C^{-1})
h_t	Heat transfer coefficient to ambient in loop.	(J s^{-1} m^{-2}°C^{-1})
h_{ext}	Heat transfer coefficient between the heat exchanger in bubble column and culture temperature	(J s^{-1} m^{-2}°C^{-1})
I_0	Incident light intensity	(W m^{-2})
I_{PFD}	Photon flux density	(μ molm^{-2}s^{-1})
K_a	Spectrally averaged absorption coefficient of algae	(m^2kg^{-1})
L	Distance	(m)
PAR	Photosynthetic active radiation	(%)
P_m^c	Maximum carbon specific rate of photosynthesis	(s^{-1})
Q_w	Volumetric flow rate of water crossing through heat exchanger	(m^3 s^{-1})
$Q_{liq,c}$	Volumetric flow rate liquid bubble column	(m^3 s^{-1})
$Q_{liq,l}$	Volumetric flow rate of liquid in loop	(m^3 s^{-1})
r_m	Maintenance metabolic coefficient	(s^{-1})
S_b	Column area available	(m^2)
S_{ext}	Heat exchanger area	(m^2)
t	Time	(h)
T	Temperature of culture	(°C)
T_{amb}	Ambient temperature	(°C)
T_{in}	Culture temperature at inlet of bubble column	(°C)
T_{let}	Lethal temperature	(°C)
T_{opt}	Optimal temperature	(°C)
T_{out}	Culture temperature at outlet of bubble column	(°C)
T_{ext}	Temperature in heat exchanger	(°C)
v	Liquid velocity	(m s^{-1})
$V_{liq,c}$	Liquid bubble column	(m^3)
V_{ext}	Heat exchanger volume	(L)

Subscripts	Description
Amb	Ambient
B	Bubble column
Ext	Heat exchanger
L	Loop
Liq	Liquid
Let	Lethal
Max	Maximum
Opt	Optimal
Out	Outlet of bubble column
PFD	Photon Flux Density

Greek letter	Description	Unit
α_t	Distribution solar factor for solar receiver	(-)
α_b	Distribution solar factor for the bubble column	(-)
$ß_T$	Curve modulating constant	(-)
σ	Functional cross section of the photosynthesis apparatus	(g C (mol^{-1} photons) m^{2}g^{-1}Chla)
μ	Growth rate	(s^{-1})
μ_{growth}	Specific growth rate	(s^{-1})
μ_{max}	Maximal growth rate	(s^{-1})
Θ	Chlorophyll a and carbon ratio in the cell	(g^{-1}Chl a g^{-1} C)
Θ_{max}	Maximal chlorophyll a and carbon ratio	(g^{-1}Chl a g^{-1} C)
ρ	Volumetric mass density	(kg m^{-3})

D. Reference for the temperature ranges in scenario.

The temperature range of the scenarios for different seasons is based on data from Yr (Merologiskinstiutt). Yr is a joint service by the Norwegian Meteorological Institute and the Norwegian Broadcasting Corporation. It gives statistics over one year about the average temperature per month and the precipitation. For the location Amsterdam, North Holland (the Netherlands) Figure D-1 and Table D-1 give the temperatures and precipitation per month. For the location Almeria, Andalucía (Spain) Figure D-2 and Table D-2 are used. It should be noted, that the weather station of Almeria is 20 metres above sea level and 37.0 km away from Almeria. The graph and table are obtained from the following website : https://www.yr.no/place/Nederland/Nord-Holland/Amsterdam/statistics.html for the Netherlands for Spain: https://www.yr.no/place/Spain/Andaluc%C3%ADa/Almer%C3%ADa/statistics.html

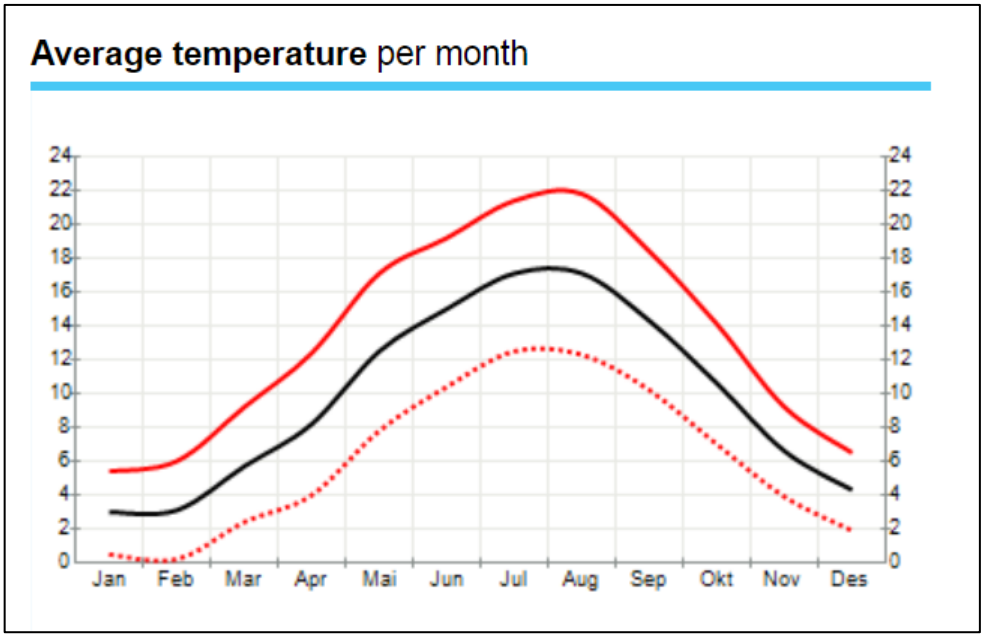

Figure D-1: Average temperature per month for the location Amsterdam, North Holland (the Netherlands).

Table D-1: Temperature and precipitation per month given the normal, warmest, coldest temperature for the location Amsterdam, North Holland (the Netherlands)

Tabular view for temperature and precipitation per month

	Temperature			Precipitation
Months	**Normal**	**Warmest**	**Coldest**	**Normal**
January	3.0°C	5.4°C	0.5°C	12
February	3.1°C	6.0°C	0.2°C	9
March	5.7°C	9.2°C	2.4°C	11
April	8.2°C	12.4°C	4.0°C	9
May	12.5°C	17.1°C	7.8°C	9
June	15.0°C	19.2°C	10.4°C	10
July	17.1°C	21.4°C	12.5°C	10
August	17.1°C	21.8°C	12.3°C	9
September	14.3°C	18.4°C	10.2°C	11
October	10.6°C	14.1°C	7.0°C	12
November	6.6°C	9.2°C	3.9°C	14
December	4.3°C	6.5°C	1.9°C	13

From this table and graph, the following conclusions were draw when it comes to the temperature range for the location Amsterdam, North Holland (the Netherlands). For the season spring (March, April, May) the temperature range is 2 – 17 °C, for the season summer (June, July, August) the temperature range is 10 – 22 °C and for the season fall (September, October, November) the temperature range is 4 – 14 °C.

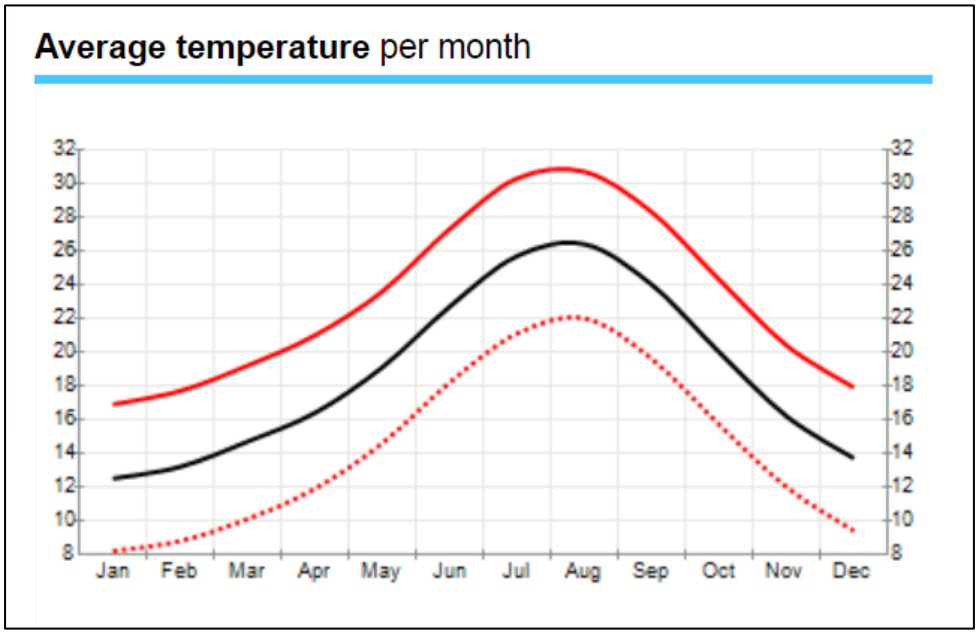

Figure D-2: Average temperature per month for the location Almeria, Andalucía (Spain)

Table D-2: Temperature and precipitation per month given the normal, warmest, coldest temperature for the location Almeria, Andalucía (Spain)

Tabular view for temperature and precipitation per month

	Temperature			Precipitation
Months	**Normal**	**Warmest**	**Coldest**	**Normal**
January	12.5°C	16.9°C	8.2°C	3
February	13.2°C	17.7°C	8.8°C	3
March	14.7°C	19.2°C	10.1°C	3
April	16.4°C	21.0°C	11.9°C	3
May	19.1°C	23.6°C	14.6°C	2
June	22.7°C	27.3°C	18.2°C	1
July	25.7°C	30.3°C	21.1°C	0
August	26.4°C	30.7°C	22.0°C	0
September	24.0°C	28.3°C	19.6°C	1
October	20.0°C	24.3°C	15.7°C	3
November	16.2°C	20.4°C	12.0°C	3
December	13.7°C	17.9°C	9.4°C	3

From this table and graph, the following conclusions were draw when it comes to the temperature range for the location Almeria, Andalucía (Spain). For the season spring (March, April, May) the temperature range is 10 – 24 °C, for the season summer (June, July, August) the temperature range is 18 – 31 °C and for the season fall (September, October, November) the temperature range is 12 – 29 °C.

E. Result of Tomlab with different start values.

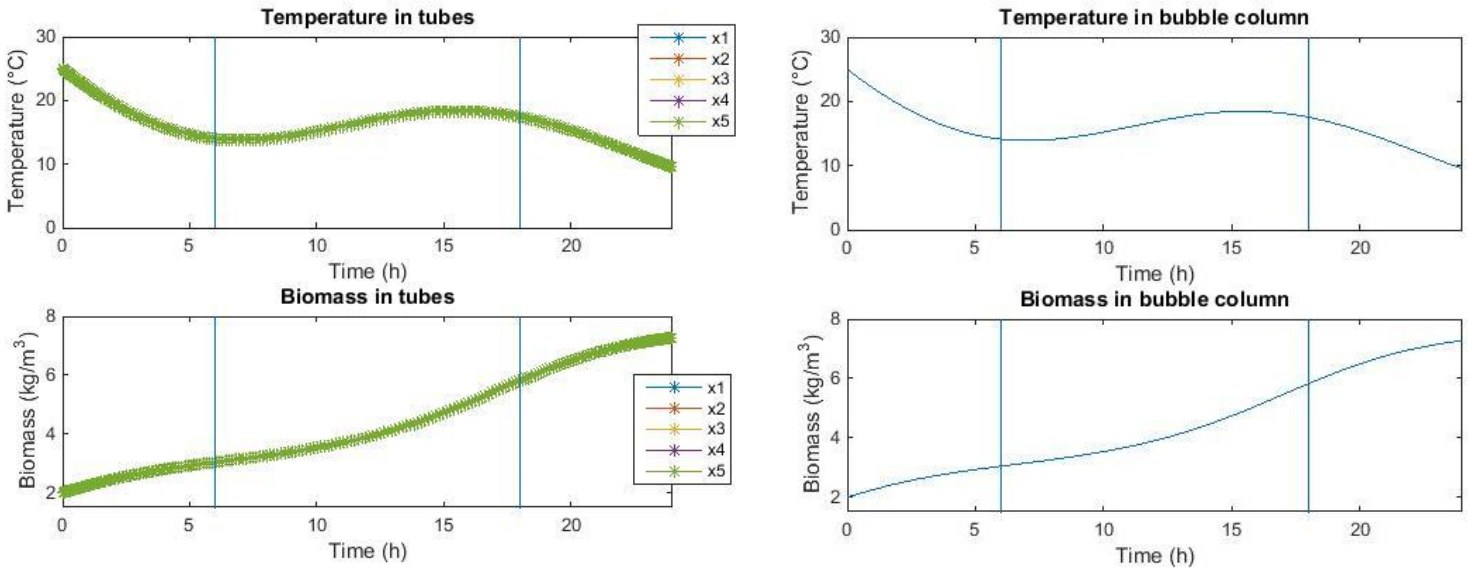

Figure E-1: Temperature change and biomass concentration in tubes (left) and in the bubble column (right), with different start values for the control input and temperature, simulated by Tomlab over one day, with the disturbance inputs being temperature range of 10-20 °C and a light intensity of 400 W/m^2 together with TSR at 6:00 and TSD at 18:00 (indicate by the vertical lines).

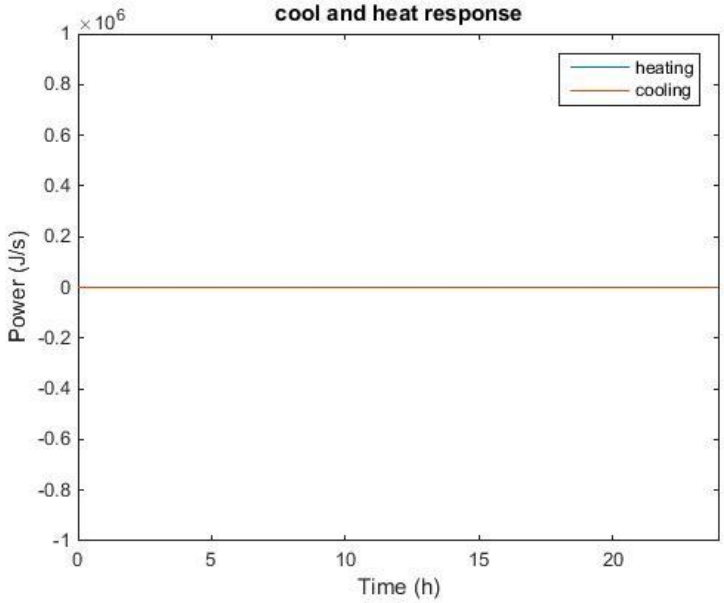

Figure E-2: Control input trajectory of Tomlab for the reference system, with different start values

```
Problem type appears to be: lpcon
Time for symbolic processing: 4.2612 seconds
Starting numeric solver
===== * * * ========================================================================== * * *
TOMLAB - Wageningen University Ac. department  705007. Valid to 2100-01-01
================================================================================================
Problem: ---  1: Temperature control            f_k      -96.568052164225776000
                                        sum(|constr|)        0.000000012964160175
                                f(x_k) + sum(|constr|)     -96.568052151261611000
                                              f(x_0)     -14.433415552745412000

Solver: snopt.  EXIT=0.  INFORM=1.
SNOPT 7.2-12 NLP code
Optimality conditions satisfied
```

Figure E-3: Outcome of the cost function (Tomlab 3.2) with different start values.

F. Code Tomlab

```
 %% Optimal control problem, tomlab
% pseudo applied, no heat exchanger equal
% lambert-beer equation added
% new differential equation to remove the biomass concentration at the end
% of the day.

%%
% define tomSym variable t (time) and tf (fixed final time)
n_day = 1;                          % amount of days
toms t; tf = n_day*24*3600;         % Fixed final time (in seconds)

% Variables to collect intermediate results:
J = []; sumc = []; cpu = [];
n = 32*8;                           % amount of collocation points.
nt = 5 ;                            % tube is divided into 5 pieces.
% Define & set time axis
tp = tomPhase('tp', t, 0, tf, n); setPhase(tp);

% Define the state and control vector; n =5;
% tomStates x1 x2 x3 x4 x5          % temperature in tubes
% tomStates x6 x7 x8 x9 x10         % biomass in tubes
% tomStates x11 x12                 % Tbubble, Cx bubble
tomStates x1 x2 x3 x4 x5 x6 x7 x8 x9 x10 x11 x12 x13 x14
tomControls u1 u2

x = [x1;x2;x3;x4;x5;x6;x7;x8;x9;x10;x11;x12;x13;x14];
%% Initial state
xi = [15;15;15;15;15;2;2;2;2;2;15;2;0;0];
x0 = {icollocate(x == xi)
    collocate({u1 == 3e3; u2 == 0})};

%% model parameters
model_parameters_final

%% control inputs
length1 = 80;
Q_liq = 5e-03;                      % volumetric flow rate of liquid in loop
[m3/s]
Q_w = 5e-04;                        % volumetric flow of water crossing in heat
exchanger       [m3/s]

% Dilution rate
F = Q_liq;                          % Flow
V = V_liq/nt;                       % volume
D = F/V;                            % diluation rate

%% disturbances inputs
ac = 0.2690;                        % spectrally averaged light absorption
coefficient          [m2/g]      [slegers]
tsu = 6*3600;
tsd = 18*3600;
tff = (24*3600-tsd + tsu);

rec_f = 4.57*0.43;
Iin = 400 * rec_f;
T_w = 10;
```

```
E0 = Iin*(sin((pi/tff)*(t-tsu)));
for i = 1:length(E0)
    ifThenElse(E0(i)<0,0,E0(i));
end

Tamb = T_w + 10*sin((pi/tff)*(t-tsu));
for i = 1:length(Tamb)
    ifThenElse(Tamb(i)<T_w,T_w,Tamb(i));
end

%% biomass tubes
% T1 with Cx1 (x1 en x6)
% Lambert - Beer
% Eaverage = E0 *((1-exp(-alpha*Xdw*B))/(alpha*Xdw*B));
li11 = E0*((1-exp(ac*x6*-d_t/2))/(ac*x6*d_t/2));

y11 = ifThenElse(x1>T_let,T_let,x1);
f_T11 = ((T_let - y11)/(T_let - T_opt))^beta_T * exp(-beta_T *((T_let -
y11)/(T_let - T_opt)-1));
P_m_c11 = mu_max*f_T11 + r_m ;
theta11 = theta_max * (1/(1 + (theta_max*alpha_photo*li11*a)/(2*P_m_c11)));
mu_growth11 = P_m_c11 * (1-exp((-alpha_photo*li11.*a*theta11)/P_m_c11));

% T2 with Cx2 (x2 en x7)
li12 = E0*((1-exp(ac*x7*-d_t/2))/(ac*x7*d_t/2));

y12 = ifThenElse(x2>T_let,T_let,x2);
f_T12 = ((T_let - y12)/(T_let - T_opt))^beta_T * exp(-beta_T *((T_let -
y12)/(T_let - T_opt)-1));
P_m_c12 = mu_max*f_T12 + r_m ;
theta12 = theta_max * (1/(1 + (theta_max*alpha_photo*li12*a)/(2*P_m_c12)));
mu_growth12 = P_m_c12 * (1-exp((-alpha_photo*li12.*a*theta12)/P_m_c12));

% T3 with Cx3 (x3 en x8)
li13 = E0*((1-exp(ac*x8*-d_t/2))/(ac*x8*d_t/2));

y13 = ifThenElse(x3>T_let,T_let,x3);
f_T13 = ((T_let - y13)/(T_let - T_opt))^beta_T * exp(-beta_T *((T_let -
y13)/(T_let - T_opt)-1));
P_m_c13 = mu_max*f_T13 + r_m ;
theta13 = theta_max * (1/(1 + (theta_max*alpha_photo*li13*a)/(2*P_m_c13)));
mu_growth13 = P_m_c13 * (1-exp((-alpha_photo*li13.*a*theta13)/P_m_c13));

% T4 with Cx4 (x4 en x9)
li14 = E0*((1-exp(ac*x9*-d_t/2))/(ac*x9*d_t/2));

y14 = ifThenElse(x4>T_let,T_let,x4);
f_T14 = ((T_let - y14)/(T_let - T_opt))^beta_T * exp(-beta_T *((T_let -
y14)/(T_let - T_opt)-1));
P_m_c14 = mu_max*f_T14 + r_m ;
theta14 = theta_max * (1/(1 + (theta_max*alpha_photo*li14*a)/(2*P_m_c14)));
mu_growth14 = P_m_c14 * (1-exp((-alpha_photo*li14.*a*theta14)/P_m_c14));

% T5 with Cx5 (x5 en x10)
li15 = E0*((1-exp(ac*x10*-d_t/2))/(ac*x10*d_t/2));

y15 = ifThenElse(x5>T_let,T_let,x5);
f_T15 = ((T_let - y15)/(T_let - T_opt))^beta_T * exp(-beta_T *((T_let -
y15)/(T_let - T_opt)-1));
```

```
P_m_c15 = mu_max*f_T15 + r_m ;
theta15 = theta_max * (1/(1 + (theta_max*alpha_photo*li15*a)/(2*P_m_c15)));
mu_growth15 = P_m_c15 * (1-exp((-alpha_photo*li15.*a*theta15)/P_m_c15));

%% temperature bubble column
% Q_heat = u1;
% Q_cool = u2;

%% biomass bubble column
% Lambert - Beer
% Eaverage = E0 *((1-exp(-alpha*Xdw*B))/(alpha*Xdw*B));
li2 = E0*((1-exp(ac*x12*-d_b/2))/(ac*x12*d_b/2));

y2 = ifThenElse(x11>T_let,T_let,x11);
f_T2 = ((T_let - y2)/(T_let - T_opt))^beta_T * exp(-beta_T *((T_let -
y2)/(T_let - T_opt)-1));
P_m_c2 = mu_max*f_T2 + r_m ;
[theta2] = theta_max * (1/(1 + (theta_max*alpha_photo*li2*a)/(2*P_m_c2)));
mu_growth2 = P_m_c2 *(1-exp((-alpha_photo*li2.*a*theta2)/P_m_c2));

%% Tomlab equality constraints: ceq

% cost cooling and heating
cost_c = 0.02;
cost_h = 0.04;
% weighting factors, cooling and heating.
w1 = 1; w2 = 1;

ceq = collocate({
    dot(x1) == (-Q_liq*rho*Cp*((x1-x11)/delta_x) +
alpha_t*li11*a*pi*d_t*delta_x - h_t*pi*d_t*delta_x*(x1-
Tamb))/(Cp*pi*d_t^2/4*delta_x*rho);
    dot(x2) == (-Q_liq*rho*Cp*((x2-x1)/delta_x) +
alpha_t*li12*a*pi*d_t*delta_x - h_t*pi*d_t*delta_x*(x2-
Tamb))/(Cp*pi*d_t^2/4*delta_x*rho);
    dot(x3) == (-Q_liq*rho*Cp*((x3-x2)/delta_x) +
alpha_t*li13*a*pi*d_t*delta_x - h_t*pi*d_t*delta_x*(x3-
Tamb))/(Cp*pi*d_t^2/4*delta_x*rho);
    dot(x4) == (-Q_liq*rho*Cp*((x4-x3)/delta_x) +
alpha_t*li14*a*pi*d_t*delta_x - h_t*pi*d_t*delta_x*(x4-
Tamb))/(Cp*pi*d_t^2/4*delta_x*rho);
    dot(x5) == (-Q_liq*rho*Cp*((x5-x4)/delta_x) +
alpha_t*li15*a*pi*d_t*delta_x - h_t*pi*d_t*delta_x*(x5-
Tamb))/(Cp*pi*d_t^2/4*delta_x*rho);
    dot(x6) == (mu_growth11-r_m)*x6 + D*(x12-x6);
    dot(x7) == (mu_growth12-r_m)*x7 + D*(x6-x7);
    dot(x8) == (mu_growth13-r_m)*x8 + D*(x7-x8);
    dot(x9) == (mu_growth14-r_m)*x9 + D*(x8-x9);
    dot(x10) ==(mu_growth15-r_m)*x10 + D*(x9-x10);

    dot(x11) == (-Q_liq*Cp*rho*(x11-x5)+ alpha_b*li2*S_b*a + h_b*S_b*(Tamb-
x11) + u1 + u2)/(Cp*rho*V_bubble);
    dot(x12) == (mu_growth2-r_m)*x12 + D*(x10-x12);

    dot(x13) == u1;
    dot(x14) == -u2;
    });

%% Boundary conditions
cbnd = initial(x ==xi);
```

```
%% Control bounds
cbox = {
        0 <= collocate(u1) <= 1e6;
        -1e6 <= collocate(u2) <= 0
        };

%% Tomlab objective to be minimized: objective
price_algae = 25;  % euro/kg
% weighting factors inside the control objective?
energy = (final(x13)*0.04 + final(x14)*0.02)/3.6e6/0.8;
objective = (-w1*price_algae*((final(x6)-2+final(x7)-2+final(x8)-
2+final(x9)-2+final(x10)-2)*V + (final(x12) -2 *V_bubble)))+ w2*energy;

%% solve the problem

options = struct;
options.name = 'Temperature control';
[solution,result] = ezsolve(objective, {cbox, cbnd, ceq}, x0, options);

% Store intermediate results: costs, nonlinear constraints, cpu time
J    = [J result.f_k];
sumc = [sumc sum(abs(result.c_k))];
cpu  = [cpu result.CPUtime];

% Obtain final solution: t, x, u
% that overwrite the associated tomSym variables
t  = subs(collocate(t),solution);
x1 = subs(collocate(x1),solution);
x2 = subs(collocate(x2),solution);
x3 = subs(collocate(x3),solution);
x4 = subs(collocate(x4),solution);
x5 = subs(collocate(x5),solution);
x6 = subs(collocate(x6),solution);
x7 = subs(collocate(x7),solution);
x8 = subs(collocate(x8),solution);
x9 = subs(collocate(x9),solution);
x10 = subs(collocate(x10),solution);
x11 = subs(collocate(x11),solution);
x12 = subs(collocate(x12),solution);
x13 = subs(collocate(x13),solution);
x14 = subs(collocate(x14),solution);
u1 = subs(collocate(u1),solution);
u2 = subs(collocate(u2),solution);

%% plot result

figure(1)
subplot(2,1,1)
plot(t/3600,x1,'*-',t/3600,x2,'*-',t/3600,x3,'*-',t/3600,x4,'*-
',t/3600,x5,'*-'); axis([0 24 0 30])
legend('x1','x2','x3','x4','x5');
xlabel('Time (h)');
ylabel('Temperature (°C)');
title('Temperature in tubes');
line([6 6], [0.1 40])
line([18 18], [0.1 40])

subplot(2,1,2)
```

```
plot(t/3600,x6,'*-',t/3600,x7,'*-',t/3600,x8,'*-',t/3600,x9,'*-
',t/3600,x10,'*-'); axis([0 24 1.5 8])
legend('x1','x2','x3','x4','x5');
xlabel('Time (h)');
ylabel('Biomass (kg/m^3)');
title('Biomass in tubes');
line([6 6], [0.1 40])
line([18 18], [0.1 40])

figure(2)
subplot(2,1,1)
plot(t/3600,x11);axis([0 24 0 30])
xlabel('Time (h)');
ylabel('Temperature (°C)');
title('Temperature in bubble column');
line([6 6], [0.1 40])
line([18 18], [0.1 40])

subplot(2,1,2)
plot(t/3600,x12); axis([0 24 1.5 8])
xlabel('Time (h)');
ylabel('Biomass (kg/m^3)');
title('Biomass in bubble column');
line([6 6], [0.1 40])
line([18 18], [0.1 40])
%%
figure(3)
plot(t/3600,u1,t/3600,u2);axis([0 24 -1e6 1e6])
legend('heating', 'cooling');
xlabel('Time (h)');
ylabel('Power (J/s)');
title('cool and heat response');
```

```
Problem type appears to be: lpcon
Time for symbolic processing: 3.8726 seconds
Starting numeric solver
===== * * * ========================================================================== * * *
TOMLAB - Wageningen University Ac. department  705007. Valid to 2100-01-01
================================================================================================
Problem: ---  1: Temperature control            f_k    -257.914961532152570000
                                        sum(|constr|)      0.000002383728799750
                                f(x_k) + sum(|constr|)   -257.914959148423750000
                                             f(x_0)    -72.167077763727107000

Solver: snopt.  EXIT=0.  INFORM=1.
SNOPT 7.2-12 NLP code
Optimality conditions satisfied

FuncEv    1 ConstrEv    7 ConJacEv    7 Iter    4 MinorIter 2773
CPU time: 72.197263 sec. Elapsed time: 71.602000 sec.
```

Figure F-1: Outcome of the cost function (tomlab 3.2)

G. Result of piecewise linear trajectories reference system

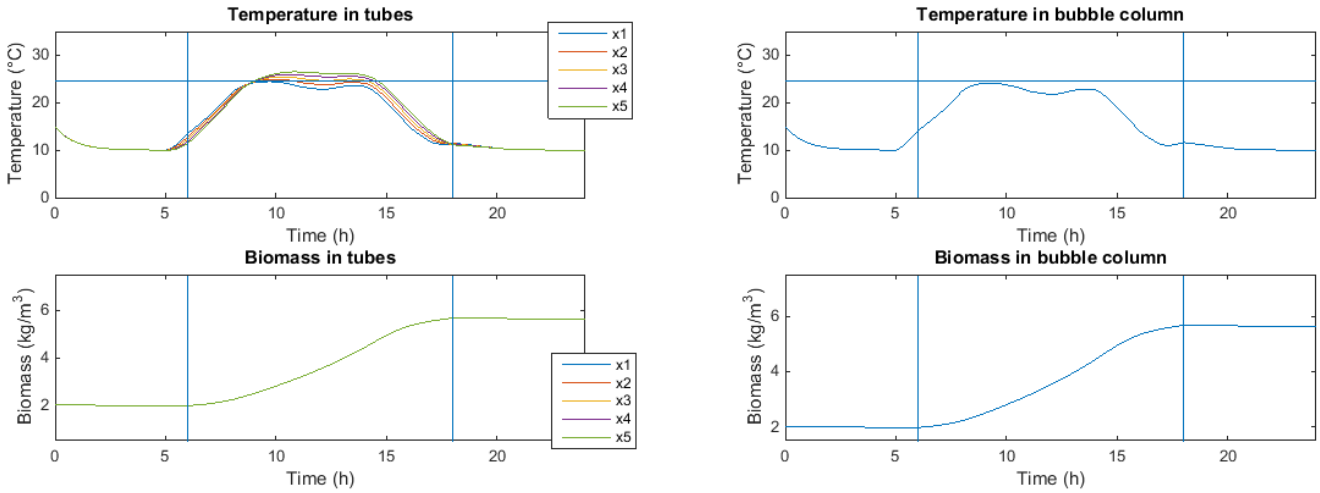

Figure G-1: Temperature change and biomass concentration in tubes (left) and in the bubble column (right) with piecewise linear trajectories over one day for the reference system (temperature range of 10-20 °C, light intensity of 400 W/m², TSR being 6:00 and TSD 18:00).

Here it is visible that it takes the system time to reach optimal temperature. The temperature is equal to the ambient temperature when TSD is reached. The microalgae growth is low when the temperature is moving up to optimal temperature. The cost for this heating and cooling trajectory are € 22,75, revenue of the microalgae € 76,20 making a profit of € 53,45. The belonging control input trajectory is given in the figure below (Figure G-2).

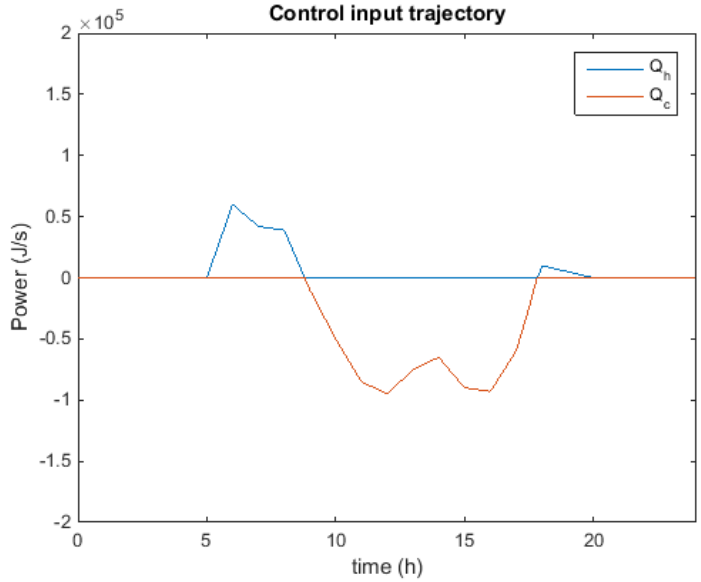

Figure G-2: Control input trajectory for the piecewise linear trajectories reference system (temperature range of 10-20 °C, light intensity of 400 W/m², TSR being 6:00 and TSD 18:00).

H. Additional figures of the scenario's location and seasons

Scenario 1.

The first scenario is the spring in Almeria (Spain) simulated, with a temperature of 10 – 24 °C and light intensity of 500 W/m^2 with TSR being 7:00 and TSD 19:00 indicated by the vertical lines. The horizontal line indicates the optimal temperature for the microalgae. In the main text the result of the tubes is shown, there the graph on the left gives the temperature change and biomass concentration in the bubble column and on the right the control input trajectory.

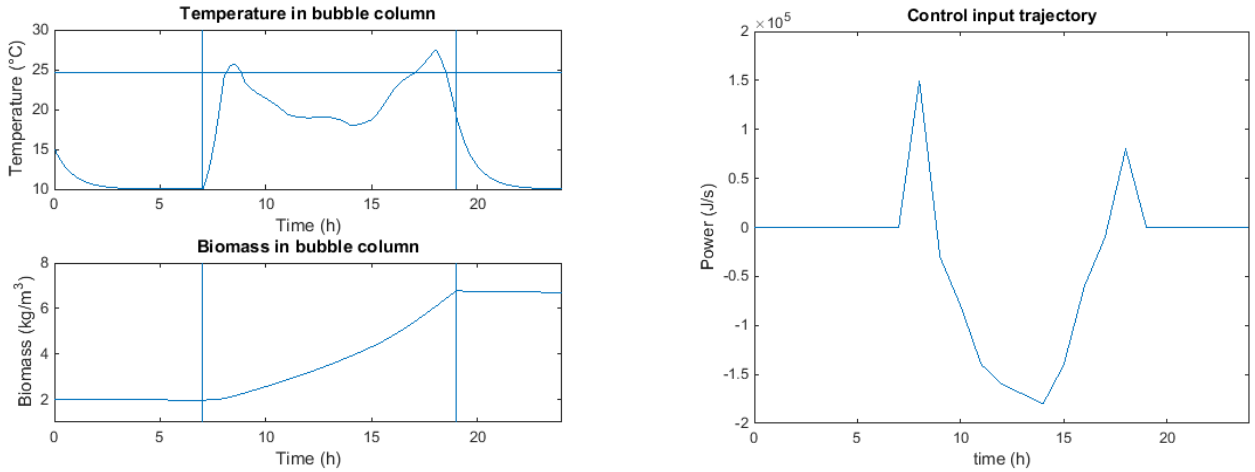

Figure H-1: Temperature change and biomass concentration in the bubble column (left) and the control input trajectory (right) simulated with piecewise linear trajectories for one day with the disturbance inputs of scenario 1

Scenario 2.

The second scenario was the summer in Almeria (Spain) simulated, with a temperature of 18 - 31 °C and light intensity of 600 W/m^2 with TSR being 7:00 and TSD 20:00 indicated by the vertical lines. The horizontal line indicates the optimal temperature for the microalgae. In the main text the result of the tubes is shown, there the graph on the left gives the temperature change and biomass concentration in the bubble column and on the right the control input trajectory.

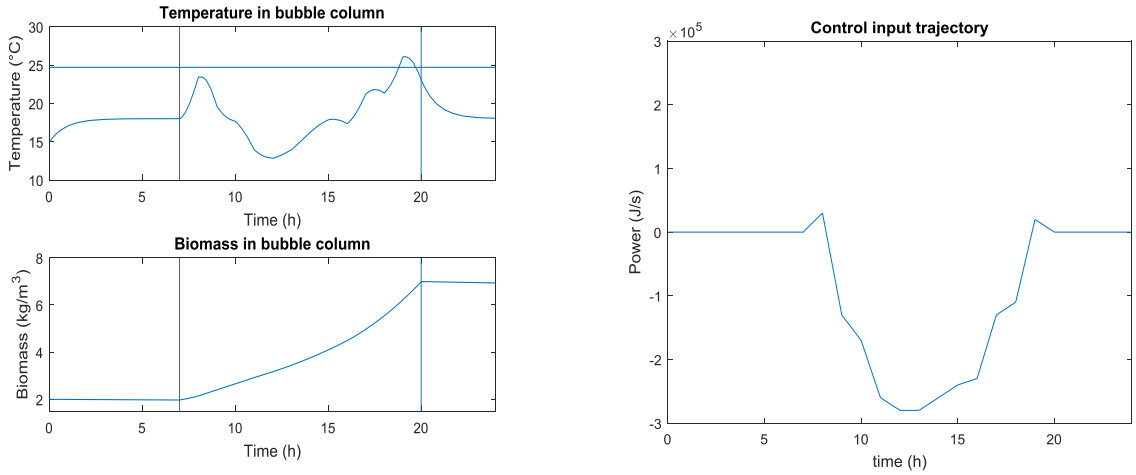

Figure H-2: Temperature change and biomass concentration in the bubble column (left) and the control input trajectory (right) simulated with piecewise linear trajectories for one day with the disturbance inputs of scenario 2

Scenario 3.

In this scenario is the fall in Almeria (Spain) simulated, with a temperature of 12 – 29 °C and light intensity of 450 W/m^2 with TSR being 7:00 and TSD 19:00 indicated by the vertical lines. The horizontal line indicates the optimal temperature for the microalgae. In the main text the result of the tubes is shown, there the graph on the left gives the temperature change and biomass concentration in the bubble column and on the right the control input trajectory.

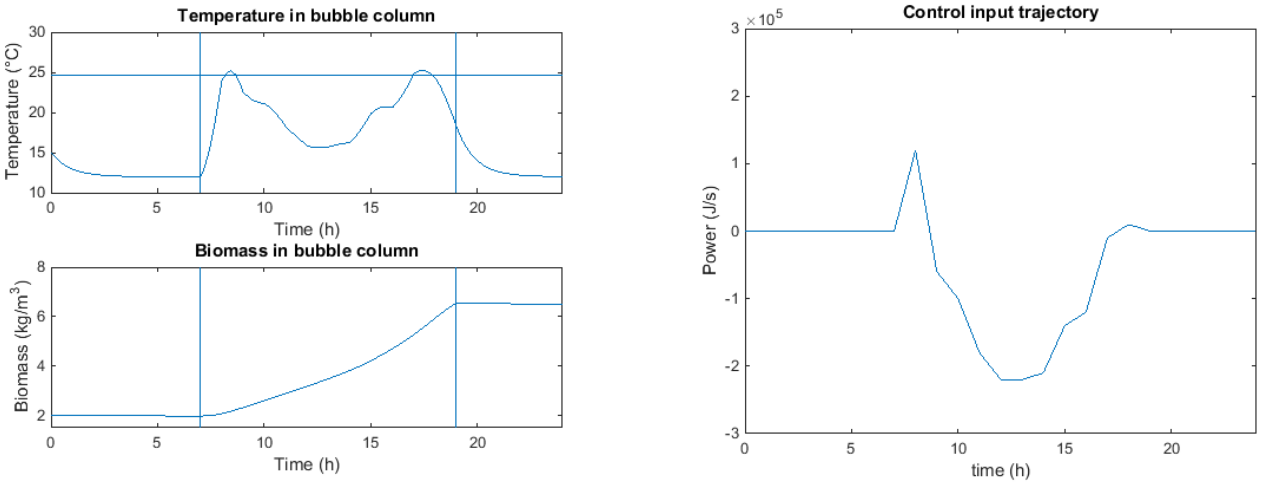

Figure H-3: Temperature change and biomass concentration in the bubble column (left) and the control input trajectory (right) simulated with piecewise linear trajectories for one day with the disturbance inputs of scenario 3

Scenario 4.

In this scenario is the spring in Amsterdam (the Netherlands) simulated, with a temperature of 2 – 17 °C and light intensity of 300 W/m^2 with TSR being 7:00 and TSD 19:00 indicated by the vertical lines. The horizontal line indicates the optimal temperature for the microalgae. In the main text the result of the tubes is shown, there the graph on the left gives the temperature change and biomass concentration in the bubble column and on the right the control input trajectory.

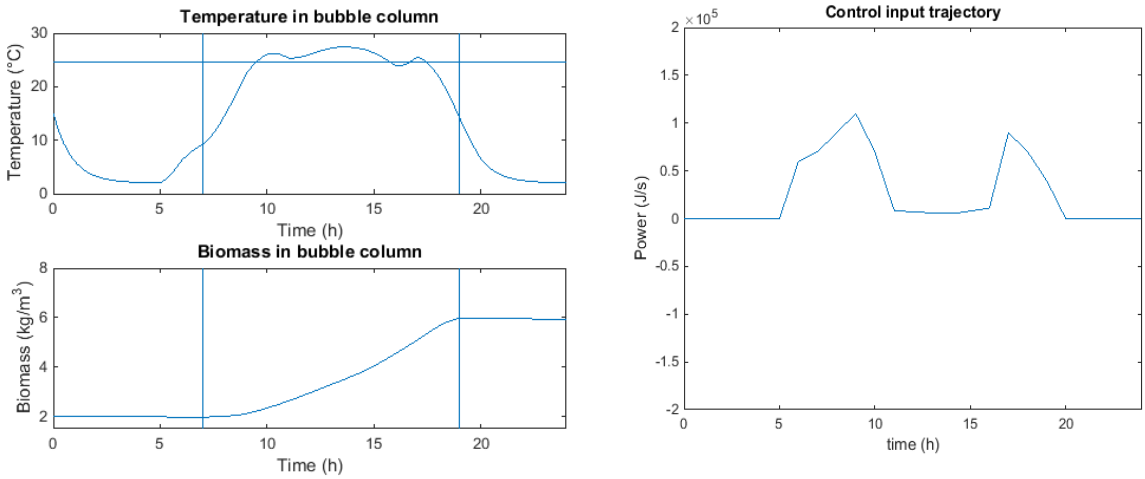

Figure H-4: Temperature change and biomass concentration in the bubble column (left) and the control input trajectory (right) simulated with piecewise linear trajectories for one day with the disturbance inputs of scenario 4

Scenario 5.

In this scenario is the summer in Amsterdam (the Netherlands) simulated, with a temperature of 10 – 22 °C and light intensity of 350 W/m^2 with TSR being 6:00 and TSD 22:00 indicated by the vertical lines. The horizontal line indicates the optimal temperature for the microalgae. In the main text the result of the tubes is shown, there the graph on the left gives the temperature change and biomass concentration in the bubble column and on the right the control input trajectory.

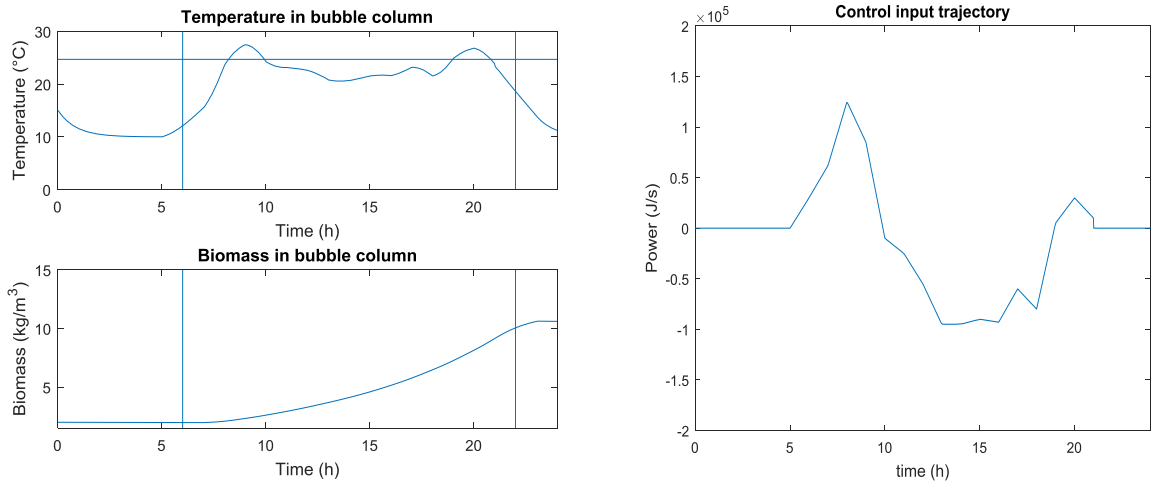

Figure H-5: Temperature change and biomass concentration in the bubble column (left) and the control input trajectory (right) simulated with piecewise linear trajectories for one day with the disturbance inputs of scenario 5

Scenario 6.

In this scenario is the fall in Amsterdam (the Netherlands) simulated, with a temperature of 4 – 14 °C and light intensity of 250 W/m^2 with TSR being 7:00 and TSD 19: 00 indicated by the vertical lines. The horizontal line indicates the optimal temperature for the microalgae. In the main text the result of the tubes is shown, there the graph on the left gives the temperature change and biomass concentration in the bubble column and on the right the control input trajectory.

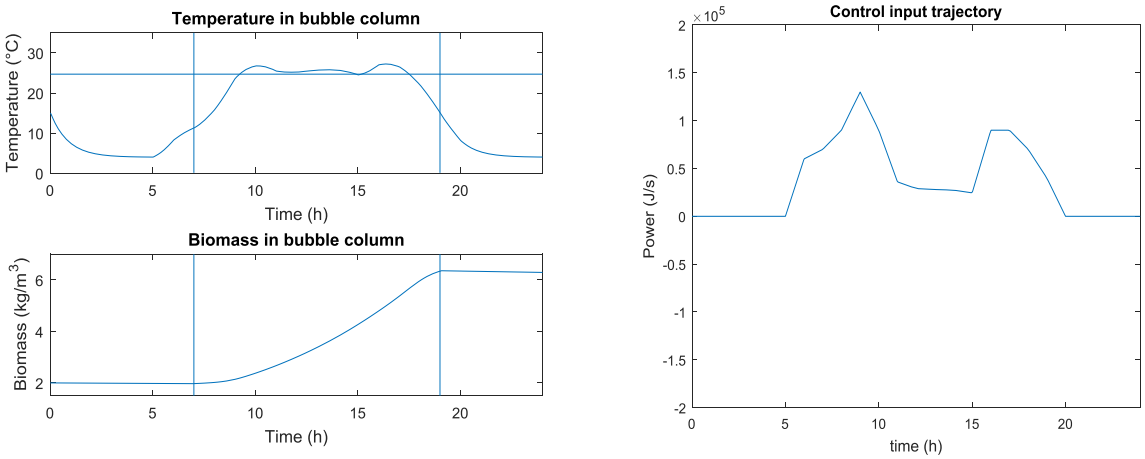

Figure H-6: Temperature change and biomass concentration in the bubble column (left) and the control input trajectory (right) simulated with piecewise linear trajectories for one day with the disturbance inputs of scenario 6